Original Research Article

PDE5 inhibitors enhance Celecoxib killing in multiple tumor types.[†]

Laurence Booth[1#], Jane L. Roberts[1#], Nichola Cruickshanks[1#], Seyedmehrad Tavallai[1#], Timothy Webb[1], Peter Samuel[1], Adam Conley[2], Brittany Binion[1], Harold F. Young[2], Andrew Poklepovic[3], Sarah Spiegel[1], and Paul Dent[1*]

Departments of Biochemistry and Molecular Biology[1], Neurosurgery[2], Medicine[3], Virginia Commonwealth University, 401 College St., Richmond, VA 23298.

Running Title: PDE5 and Celecoxib.

Abbreviations: ERK: extracellular regulated kinase; MEK: mitogen activated extracellular regulated kinase; PI3K: phosphatidyl inositol 3 kinase; MAPK: mitogen activated protein kinase; ca: constitutively active; dn: dominant negative; CMV: empty vector plasmid or virus; si: small interfering; SCR: scrambled; Ad: adenovirus; TUNEL: Terminal deoxynucleotidyl transferase UTP nick end labeling; VEH: vehicle; SIL: sildenafil; VAR: vardenafil; TAD: tadenafil; CEL: celecoxib; PDE: phosphodiesterase; NECRO: necrostatin 1; FADD: Fas-associated death domain protein; CD95: cluster of determinants 95; AIF: apoptosis inducing factor.

Support for the present study was funded from PHS grants from the National Institutes of Health [R01-CA141704, R01-CA150214, R01-DK52825, R01-CA61774]. No conflicts of interest to report.

joint first authors

*Correspondence to:
Paul Dent
401 College Street
Massey Cancer Center, Box 980035
Department of Biochemistry and Molecular Biology
Virginia Commonwealth University
Richmond VA 23298-0035.
Tel: 804 628 0861
Fax: 804 827 1014
pdent@vcu.edu

[†]This article has been accepted for publication and undergone full peer review but has not been through the copyediting, typesetting, pagination and proofreading process, which may lead to differences between this version and the Version of Record. Please cite this article as doi: [10.1002/jcp.24843]

Additional Supporting Information may be found in the online version of this article.

Received 15 September 2014; Revised; Accepted 2 October 2014
Journal of Cellular Physiology
© 2014 Wiley Periodicals, Inc.
DOI 10.1002/jcp.24843

Accepted Article

Abstract

The present studies determined whether clinically relevant phosphodiesterase 5 (PDE5) inhibitors interacted with a clinically relevant NSAID, celecoxib, to kill tumor cells. Celecoxib and PDE5 inhibitors interacted in a greater than additive fashion to kill multiple tumor cell types. Celecoxib and sildenafil killed ex vivo primary human glioma cells as well as their associated activated microglia. Knock down of PDE5 recapitulated the effects of PDE5 inhibitor treatment; the nitric oxide synthase inhibitor L-NAME suppressed drug combination toxicity. The effects of celecoxib were COX2 independent. Over-expression of c-FLIP-s or knock down of CD95 / FADD significantly reduced killing by the drug combination. CD95 activation was dependent on nitric oxide and ceramide signaling. CD95 signaling activated the JNK pathway and inhibition of JNK suppressed cell killing. The drug combination inactivated mTOR and increased the levels of autophagy and knock down of Beclin1 or ATG5 strongly suppressed killing by the drug combination. The drug combination caused an ER stress response; knock down of IRE1α/XBP1 enhanced killing whereas knock down of eIF2α/ATF4/CHOP suppressed killing. Sildenafil and celecoxib treatment suppressed the growth of mammary tumors in vivo. Collectively our data demonstrate that clinically achievable concentrations of celecoxib and sildenafil have the potential to be a new therapeutic approach for cancer.

Key Words: Celebrex, Viagra, cancer therapy

Accepted Article

Accepted Article

Introduction

Cyclooxygenase 2 (COX2) is one of three prostaglandin endoperoxide synthase enzymes which convert arachidonic acid to prostaglandins, leading to an inflammatory response (Nandakishore et al, 2014; Chandrasekharan et al, 2002; Vosooghi and Amini, 2014). Inhibition of COX1-3 will thus tend to suppress inflammation and a variety of well-established non-steroidal anti-inflammatory drugs such as aspirin and ibuprofen act to block these enzymes (Flower, 2003). More recently developed NSAID drugs have a greater degree of specificity for COX2 over COX1, potentially reducing systemic toxicity due to a lack of COX1 inhibition; drugs such as celecoxib (trade mark, Celebrex) (Hsieh et al, 2008; Swiergiel and Dunn, 2002).

COX2 is over-expressed in several tumor types and drugs that inhibit COX2 i.e. celecoxib, can cause in a dose-dependent fashion, tumor cell killing (Johnson et al, 2001; Hsu et al, 2000; Williams et al, 2000). However, in many studies the in vitro doses of celecoxib used to kill tumor cells are above those achievable in human *tissues* after a 200-800 mg drug dose i.e. ~2.5-7.5 μM (Werner et al, 2002; see http://dailymed.nlm.nih.gov/). There is also solid evidence that COX2 inhibitors have cancer chemo-preventative actions in patients e.g. colorectal polyps using 400 mg BID (Saba et al, 2013; Kim and Giardiello, 2011; Mao et al, 2011). However, although drugs such as celecoxib have anti-cancer effects it has been observed that tumor cells exhibiting low levels of COX2 can exhibit sensitivity to these agents, arguing that COX2 inhibitors are likely to have multiple COX2-independent cellular targets in terms of their effects on cancer biology (Bastos-Pereira et al, 2010; Schiffmann et al, 2008; Chuang et al, 2008; Grosch et al, 2001). The reported mechanisms by which COX2 inhibitors regulate tumor cell viability are diverse and include altered levels of autophagy and endoplasmic reticulum stress signaling; increased death receptor expression and reduced levels of c-FLIP-s; inhibition of the AKT protein kinase; modulation of PPARγ function; increased mitochondrial injury and down-regulation of protective BCL-2 family proteins; ceramide generation; and activation of protein kinase G (PKG) (Huang et al,

2013; Pyrko et al, 2007; Liu et al, 2004; Ramer et al, 2013; Piplani et al, 2013; Song et al, 2013; Chen et al, 2011; Schiffmann et al, 2010; Soh et al, 2008).

Phosphodiesterase 5 (PDE5) inhibitors were originally developed as agents to manipulate cardio-vascular biology that were in parallel noted to treat erectile dysfunction (Watanabe et al, 2002; Bruzziches et al, 2013). Inhibition of PDE5 suppresses the degradation of cyclic GMP resulting in the activation of PKG (Francis et al, 2010). cGMP/PKG, through its stimulatory actions upon the ERK, p38 MAPK, JNK and NFκB pathways can increase the expression of inducible nitric oxide synthase (iNOS), resulting in the production of nitric oxide (NO) (Komalavilas et al, 1999; Das et al, 2008; Choi et al, 2009). NO and cGMP/PKG have multiple cellular targets including (to name but a few) ion channels, receptors, phospholipases, Rho A, altered protein nitrosylation, ceramide generation and death receptor signaling (Francis et al, 2010; Florio et al, 2003; Russwurm et al, 2013; Kots et al, 2011; Hayden et al, 2001).

Prior studies from our laboratories have demonstrated that PDE5 inhibitors enhance the toxicities of multiple well established cytotoxic chemotherapies (Booth et al, 2014; Das et al, 2010; Roberts et al, 2014). In these studies PDE5 inhibitors, in an NOS-dependent fashion, were show to enhance chemotherapy killing through activation of the CD95 death receptor pathway, the generation of reactive oxygen species and mitochondrial dysfunction. The mechanism(s) by which PDE5 inhibitors and chemotherapies interacted to activate CD95 were not further explored.

The present studies grew out of those described in refs. (Booth et al, 2014; Das et al, 2010; Roberts et al, 2014), and were designed to determine whether PDE5 inhibitors enhanced celecoxib toxicity in tumor cells and if so, the molecular mechanisms by which the drugs interact. PDE5 inhibitors and celecoxib, in an NOS-dependent

Accepted Article

and COX2-independent fashion, killed multiple tumor cell types, including tumor stem cells and anoikis resistant tumor cells. Cell killing required expression of the death receptor CD95, though tyrosine phosphorylation of the receptor was not required for the death signal. The drug combination induced ER stress signaling and autophagy that were both causal in tumor cell killing.

Materials and Methods.

Materials.

Phospho-/total- antibodies were purchased from Cell Signaling Technologies (Danvers, MA) and Santa Cruz Biotech. (Santa Cruz, CA). All drugs were purchased from Selleckchem (Houston, TX). Commercially available validated short hairpin RNA molecules to knock down RNA / protein levels were from Qiagen (Valencia, CA). Antibody reagents, other kinase inhibitors, caspase inhibitors cell culture reagents, and non-commercial recombinant adenoviruses have been previously described (Cruickshanks et al, 2013; Tang et al, 2012; Park et al, 2010). Previously characterized semi-established GBM5 / GBM6 / GBM12 / GBM14 glioblastoma cells were supplied by Dr. C.D. James (University of California, San Francisco) and Dr. J.N. Sarkaria (Mayo Clinic, Rochester MN) and were not further characterized by ourselves (Giannini et al, 2005). The primary human GBM isolates (patient 1; patient 2; patient 3) and primary human medulloblastoma isolates (HOSS1, VC312, CON1) were obtained / isolated from discarded tumor tissue after standard of care surgery. Patients had previously given informed consent under an IRB protocol to the use of tumor tissue. Tumor samples were made anonymous of all patient identifiers by the VCU TDAAC prior to hand-over to the Dent laboratory.

Methods.

Cell culture and in vitro exposure of cells to drugs. All fully established cancer lines were cultured at 37 ^{o}C (5% (v/v CO_2) *in vitro* using RPMI supplemented with 10% (v/v) fetal calf serum and 10% (v/v) Non-

Accepted Article

essential amino acids. All primary human GBM cells were cultured at 37 ^{o}C (5% (v/v CO_2) *in vitro* using RPMI supplemented with 2% (v/v) fetal calf serum and 10% (v/v) Non-essential amino acids. at 37 ^{o}C (5% (v/v CO_2). GBM5/6/12/14 stem cells were cultured in StemCell Technologies NeuroCult NS-A Basal Medium supplemented with 20 μg/ml bFGF, 20 μg/ml EGF and 2 mM heparin. For short-term cell killing assays and immunoblotting, cells were plated at a density of 3 x 10^3 per cm^2 and 24h after plating were treated with various drugs, as indicated. *In vitro* small molecule inhibitor treatments were from a 100 mM stock solution of each drug and the maximal concentration of Vehicle (DMSO) in media was 0.02% (v/v). Cells were not cultured in reduced serum media during any study.

Cell treatments, SDS-PAGE and Western blot analysis. Cells were treated with various drug concentrations, as indicated in the Figure legends. Samples were isolated at the indicated times and SDS PAGE and immunoblotting was performed as described in refs (Cruickshanks et al, 2013; Tang et al, 2012; Park et al, 2010). Blots were observed by using an Odyssey IR imaging system (LI-COR Biosciences, Lincoln, NE).

Recombinant adenoviral vectors; infection in vitro. We generated and purchased previously noted recombinant adenoviruses as per refs. (Cruickshanks et al, 2013; Tang et al, 2012; Park et al, 2010). Cells were infected with these adenoviruses at an approximate m.o.i. as indicated in the Figure / Legend (usually an moi of 50). Cells were incubated for 24 h to ensure adequate expression of transduced gene products prior to drug exposures.

Detection of cell death by Trypan Blue assay. Cells were harvested by trypsinization with Trypsin/EDTA for ~10 min at 37 ^{o}C. Harvested cells were combined with the culture media containing unattached cells and the mixture centrifuged (800 rpm, 5 min). Cell pellets were resuspended in PBS and mixed with trypan blue agent.

Accepted Article

Viability was determined microscopically using a hemocytometer (Cruickshanks et al, 2013; Tang et al, 2012; Park et al, 2010). Five hundred cells from randomly chosen fields were counted and the number of dead cells was counted and expressed as a percentage of the total number of cells counted. Cell killing was confirmed using the *Sceptor* instrument (Millipore, Billerica MA) with a 60 μm tip, which measured tumor cell size/sub G1 DNA as an indication of tumor cell viability.

Soft agar colony formation assay. Tumor cells were triturated to form single cells and were plated into soft agar in sextuplicate using established procedures (500-1000 cells per 60 mm dish) (Cruickshanks et al, 2013). Cells were treated with vehicle (DMSO), Celecoxib (5.0 μM), sildenafil (as indicated, μM) or the drugs combined. Twenty four h after drug treatment the plates were washed with drug free media and the cover media was replaced with drug free media. Colonies were permitted to form over the following 20 days, after which they were stained and colonies counted.

Assessment of autophagy. Cells were transfected with a plasmid to express a green fluorescent protein (GFP) and red fluorescent protein (RFP) tagged form of LC3 (ATG8). For analysis of cells transfected with the GFP-RFP-LC3 construct, the GFP/RFP -positive vesicularized cells were examined under the X40 objective of a Zeiss Axiovert fluorescent microscope.

Plasmid transfection.

Plasmids: Cells were plated as described above and 24 h after plating, transfected. Plasmids (0.5 μg) expressing a specific mRNA or appropriate vector control plasmid DNA was diluted in 50 μl serum-free and antibiotic-free medium (1 portion for each sample). Concurrently, 2 μl Lipofectamine 2000 (Invitrogen), was diluted into 50 μl of serum-free and antibiotic-free medium. Diluted DNA was added to the diluted Lipofectamine 2000 for each sample and incubated at room temperature for 30 min. This mixture was

Accepted Article

added to each well/dish of cells containing 200 µl serum-free and antibiotic-free medium for a total volume of 300 µl and the cells were incubated for 4h at 37^{o}C. An equal volume of 2X medium was then added to each well. Cells were incubated for 48h, then treated with drugs. To assess transfection efficiency of plasmids we used a plasmid to express GFP and defined the percentage of cells being infected as the percentage of GFP+ cells. For all cell lines the infection efficiency was > 70%.

siRNA: Cells were plated in 60 mm dishes from a fresh culture growing in log phase as described above, and 24h after plating transfected. Prior to transfection, the medium was aspirated and 1 ml serum-free medium was added to each plate. For transfection, 10 nM of the annealed siRNA, the positive sense control doubled stranded siRNA targeting GAPDH or the negative control (a "scrambled" sequence with no significant homology to any known gene sequences from mouse, rat or human cell lines) were used (predominantly Qiagen, Valencia, CA; occasional alternate siRNA molecules were purchased from Ambion, Inc., Austin, Texas). Ten nM siRNA (scrambled or experimental) was diluted in serum-free media. Four µl Hiperfect (Qiagen) was added to this mixture and the solution was mixed by pipetting up and down several times. This solution was incubated at room temp for 10 min, then added drop-wise to each dish. The medium in each dish was swirled gently to mix, then incubated at 37 ^{o}C for 2h. One ml of 10% (v/v) serum-containing medium was added to each plate, and cells were incubated at 37 ^{o}C for 24-48h before re-plating (50 x 10^3 cells each) onto 12-well plates. Cells were allowed to attach overnight, then treated with drugs (0-48h). Trypan blue exclusion assays and SDS PAGE / immunoblotting analyses were then performed at the indicated time points.

Immunohistochemistry and live-dead assays. Immunohistochemistry and live-dead assays were performed in 96 well plates using a Hermes Wiscan instrument (IDEA Bio-medical, Rehovot, Israel). Cells were plated and treated with drugs for 12-24h as indicated in the Figure / Legend. After treatment plates were centrifuged to deposit floating cells onto the plate (800 rpm, 5 min). Cells were then either fixed in place (4% paraformaldehyde in PBS) or were subjected to live-dead assay using a commercially available kit and

Accepted Article

performed according to the manufacturer's method (Life Technologies, Grand Island, NY). Cell viability was measured using Wisoft software. Fixed cells were subjected to Ki67 / IL-6 / TNFα staining using standard procedures (Park et al, 2010).

Isolation of activated microglia. Following acquisition of fresh GBM tumor tissue, we isolated activated microglia using CD11b microglia microbeads (MACS, Miltenyi Biotec., San Diego, CA). Tumor tissue was macerated and single cell suspensions obtained using a Miltenyi neural tissue dissociation kit.

Animal studies. For studies with human mammary carcinoma cells, athymic Nu/Nu mice (8 week old, female) were injected, into the 4th mammary fat pad, with 1 x 10^6 / 1 x 10^7 BT474 cells or 3 x 10^6 / 1 x 10^7 BT549 cells. Tumors of ~150 mm^3 grew over the following month. Animals were segregated into tumor volumes of approximate equivalent mean tumor size and standard error. The animals were administered vehicle diluent (cremophore), sildenafil (2.5 / 5.0 mg/kg), celecoxib (2.5, 10 or 25 mg/kg) or the drug combination by oral gavage once every day for 5 days. Other tumor studies used FTY720 (0.05 mg/kg). We performed the experiment twice (n = 2) with a total of 8 animals per treatment group. Tumor volumes are measured every two-three days as indicated.

Mass spectrometry measurements. Equal numbers of cells (5.98 +/- 0.02 x 10^6) cells were treated for 6h and lipids were extracted. Bioactive lipid levels were quantified by liquid chromatography–electrospray ionization–tandem mass spectrometry (LC-ESI-MS/MS) with a Shimadzu LC-20AD binary pump HPLC system (Shimadzu, Kyoto, Japan) and an Applied Biosystems 4000 QTRAP operating in a triple quadrupole mode, as described previously (Hait NC, et al. Science 2009; 325: 1254-1257).

Data analysis. Comparison of the effects of various treatments was performed using one way analysis of variance and a two tailed Student's *t*-test. Statistical examination of *in vivo* animal survival data utilized log

Accepted Article

rank statistical analyses between the different treatment groups. Differences with a *p*-value of < 0.05 were considered statistically significant. Experiments shown are the means of multiple individual points from multiple experiments (± SEM).

Results

Initial studies examined whether there was a toxic interaction between the PDE5 inhibitor sildenafil and the non-steroidal anti-inflammatory drug celecoxib. In mammary carcinoma cell lines growing in 10% fetal calf serum sildenafil and celecoxib interacted in a greater than additive fashion to kill parental wild type tumor cells as well as anoikis resistant variants of these cells at doses as low as 0.5 μM sildenafil and 1 μM celecoxib (Figures 1A-1C). A similar toxic interaction between sildenafil and celecoxib was observed in hepatoma, colorectal cancer, glioblastoma and medulloblastoma cells (Figures 1D and 1E; Figures S1A-S1F). Stem-like GBM12 cells and other stem-like GBM cell derivatives expressed higher levels of CD133 and other stem cell markers than parental GBM cells (Figure S1G). Not only did sildenafil and celecoxib treatment kill cells; it also profoundly reduced tumor cell proliferation as judged by reduced Ki67 staining (Figure 1F, upper IHC). In median dose effect colony formation assays sildenafil and celecoxib interacted in a greater than additive fashion to kill breast cancer cells with combination index values lower than 0.70 (Figure 1F, lower graphs). As judged by increased phosphorylation of the protein VASP-1 at S239 (a PKG site), following sildenafil treatment, we were increasing cGMP levels (Figure 1G). As judged by increased phosphorylation of the endoplasmic reticulum stress marker eIF2α, following celecoxib treatment, we were inducing an ER stress response (Figures 1H). As judged by decreased expression of the sphingosine-1-phosphate receptor 1 (EDG-1), a target of the multiple sclerosis medicine FTY720 (Fingolimod, Gilenya), FTY720 alone and [sildenafil + celecoxib] treatments reduced EDG-1 expression (Figure 1I).

Accepted Article

Studies were then performed to define on- and off-target actions of our drugs and their effects on cell viability. The chemically dissimilar PDE5 inhibitor tadalafil interacted with celecoxib to kill tumor cells (Figures 2A and 2B). We noted that the expression of PDE5 was elevated in breast, lung and liver tumor tissue compared to matched non-tumor tissues from the same organs arguing for a relatively more specific on-target effect in tumor compared to normal tissues (Figures 2C-2E). The celecoxib derivative 2,5-dimethyl celecoxib, that does not inhibit COX2, was as efficacious as celecoxib at enhancing sildenafil toxicity (Figure 2F). Knock down of COX2 did not alter the lethality of the sildenafil and celecoxib drug combination in breast cancer cells (Figure 2G). Knock down of PDE5 expression enhanced celecoxib lethality (Figure 2H). The nitric oxide synthase (NOS) inhibitor L-NG-Nitroarginine Methyl Ester (L-NAME) inhibited cell killing by sildenafil and celecoxib, consistent with the ability of PDE5 inhibitors to increase iNOS and NO production (Figures 2I and 2J). Sildenafil and celecoxib treatment radiosensitized tumor cells (Figure 2K). Collectively these findings argue that celecoxib, in a COX2 –independent fashion, promotes tumor cell killing in cells lacking PDE5 expression and does so in an NOS –dependent manner.

In Figure 1 we noted that celecoxib and sildenafil interacted to kill GBM / GBM stem-like cells as well as GBM cells freshly isolated from patients. The growth of all tumors is influenced by stromal cell signaling; in the brain activated microglia play a pivotal role in the proliferation and invasive potential of malignant glial tumors. Hence we next examined the impact of sildenafil and celecoxib treatment on activated microglia freshly isolated from GBM tumors ex vivo and on the synthesis of paracrine ligands by the activated microglia. Celecoxib and sildenafil interacted in a greater than additive fashion to kill activated microglia (Figure S2A). Treatment of activated microglia with celecoxib and sildenafil rapidly reduced expression of interleukin 6 and of tumor necrosis factor α (Figure S2B). Thus sildenafil and celecoxib treatment has the potential to kill activated stromal cells in the brain and to suppress their production of growth promoting and inflammatory cytokines.

Accepted Article

We next examined the roles signal transduction pathways play in regulating the response of tumor cells to sildenafil and celecoxib treatment. Drug combination exposure almost abolished ERK1/2 activity and reduced phosphorylation of AKT, mTOR, p70 S6K and p65 NFκB at regulatory sites (Figure 3A). Initially we made use of HCT116 colon cancer cells expressing in wild type cells a mutant active K-RAS D13 or mutant forms of H-RAS V12 that specifically activated RAF-1 or PI3K (Caron et al, 2005). Expression of H-RAS V12 protected cells from celecoxib and sildenafil toxicity to a greater extent than did expression of K-RAS D13. The protective effect of H-RAS V12 was lost in cells expressing a mutant H-RAS V12 protein that specifically activated only RAF-1 or a H-RAS V12 protein that specifically activated only PI3K (Figure 3B). In BT549 breast cancer cells which are null for phosphatase and tensin homolog (PTEN), expression of activated AKT or MEK1 significantly reduced drug combination toxicity and expression of dominant negative AKT or MEK1 enhanced drug combination lethality (Figures 3C and 3D). Expression of activated forms of p70 S6K or mTOR also suppressed drug combination killing, as did inhibition of JNK signaling (Figures 3E and 3F). Surprisingly, expression of dominant negative p38 MAPK enhanced drug toxicity. Incubation of cells with the NOS inhibitor L-NAME suppressed both sildenafil-induced and (sildenafil + celecoxib)-induced activation of JNK (Figure 3G).

We next defined the cell survival regulatory pathways by which celecoxib and sildenafil interacted to kill tumor cells. Inhibition of the intrinsic apoptosis pathway by over-expression of BCL-XL or expression of dominant negative caspase 9 reduced cell killing (Figures 4A and 4B). Of note however was that over-expression of the caspase 8 inhibitor c-FLIP-s also protected cells, suggestive that the extrinsic apoptosis pathway was being activated. In general agreement with the hypothesis that the extrinsic pathway was being activated, knock down of the docking protein FAS associated death domain (FADD) or of the death receptor CD95 attenuated the toxic interaction between sildenafil and celecoxib (Figure 4C). In further agreement with a role for CD95 in the killing process, drug combination exposure caused a rapid plasma membrane localization and clustering of CD95, indicative of receptor activation (Figure 4D). Of particular note, whilst

Accepted Article

knock down of FAS-Ligand reduced killing by ~50% use of a neutralizing anti-FAS-L antibody had no impact on cell killing, despite the antibody being able to block exogenous FAS-L killing (Figures 4E and 4F, data not shown). Thus the mechanisms by which knock down of total FAS ligand expression can alter CD95 signaling remain to be resolved. Incubation of cells with the NOS inhibitor L-NAME prevented CD95 plasma membrane localization (Figure 4G). There are multiple mechanisms by which CD95 can become activated including the actions of ceramides for receptor clustering and tyrosine phosphorylation for receptor oligomerization (Park et al, 2010; Eberle et al, 2007). To test whether tyrosine phosphorylation of CD95 played a role in sildenafil/celecoxib biology we utilized HuH7 hepatoma cells that are CD95 null together with constructs to express either wild type CD95 or a CD95 protein that lacks the two sites of regulatory tyrosine phosphorylation (CD95 Y232F Y291F) (Hamed et al, 2013). Regardless of tyrosine phosphorylation status, expression of CD95 facilitated the toxic interaction between sildenafil and celecoxib (Figure 4H).

Studies from our laboratory using the non-coxib derivative of celecoxib, OSU-03012, have shown that this compound kills tumor cells through the induction of endoplasmic reticulum (ER) stress and autophagy (Yacoub et al, 2006; Park et al, 2008; Booth et al, 2012). Initial studies to examine autophagy in the present studies made use of cells transfected to express an LC3-GFP-RFP construct. Treatment of cells with sildenafil and celecoxib increased the numbers of early autophagosome GFP+ and late RFP+ autolysosome vesicles in cells suggestive that autophagic flux was being induced (Figure 5A). Incubation of cells with the nitric oxide synthase inhibitor L-NAME suppressed the drug-induced induction of GFP+ and RFP+ vesicles (Figure 5B). Knock down of the autophagy regulatory proteins Beclin1 or ATG5 abolished the induction of autophagy and significantly reduced the toxicity of sildenafil and celecoxib treatment (Figure 5C, data not shown). We next examined the role of ER stress signaling in the cellular response to sildenafil and celecoxib treatment. Inhibition of the IRE1/XBP1 arm of the ER stress response increased the toxicity of sildenafil and celecoxib treatment (Figures 5D and 5E). Inhibition of the eIF2α/ATF4 arm of the ER stress response

Accepted Article

almost abolished the lethality of sildenafil and celecoxib treatment; knock down of CHOP had a more modest effect at reducing cell killing. The data with eIF2α knock down correlated with the drug combination causing increasing phosphorylation of eIF2α (Figure 5D, inset panel; see also data in Figure 1). Expression of a dominant negative form of eIF2α (S51A) protected cells from sildenafil and celecoxib treatment toxicity whereas expression of an activated mutant of eIF2α (S51D) enhanced drug –induced killing (Figure 5F). Inhibition of eIF2α or CD95 function (knock down) suppressed the activation of JNK caused by sildenafil and celecoxib treatment (Figure 5G (*cf* data in Figure 3F)).

The generation of ceramide species is known to play an important role in the activation of CD95 and JNK following exposure to a variety of stressful stimuli. We and others have previously shown that ceramide generation can mediate CD95 activation (Park et al, 2010). Indeed, inhibition of de-novo ceramide synthesis using fumonisin B1 reduced drug-induced activation of both CD95 and JNK, and suppressed killing by the drug combination (Figures S3A and S3B). Intriguingly, 6h after celecoxib exposure, dihydro-ceramide levels significantly increased (indicative of ceramide synthase 2 / 3 / 6 activation) (Figure S3C) and dihydro-sphingosine-1-phosphate levels were decreased (Figure S3D). Both of these changes in dihydro sphingolipids were at least partially prevented by pre-treatment with the nitric oxide synthase inhibitor L-NAME (Figures S3C-S3H). However, of particular concern was that as a single agent, celecoxib increased the levels of sphingosine-1-phosphate (Figure S3H). Knock down of ceramide synthase 6, but not ceramide synthase 2, reduced cell killing by the drug combination (Figure S3I).

Based on our data in Figure S3A-S3I, we determined whether treatment of [celecoxib + sildenafil] cells with clinically relevant FDA approved agents which also increase ceramide levels and reduce sphingosine-1-phosphate levels could further enhance the killing effect caused by [celecoxib + sildenafil]. FTY720 (Fingolimod, Gilenya) is an FDA approved drug for the treatment of multiple sclerosis that acts to suppress

Accepted Article

sphingosine-1-phosphate signaling processes as well as sphingosine-1-phosphate production and also causes an increase in ceramide levels (see data in Figure 1). FTY720 can also act as a histone deacetylase inhibitor against HDAC1 and HDAC2 and prior studies from our laboratory have shown that HDAC inhibitors increase expression of CD95 (Cruickshanks et al, 2013; Park et al, 2010). Fenretinide (4HPR) is a much trialed synthetic chemical related to vitamin A that inhibits the *desaturase* enzyme which metabolizes dihydro-ceramides, and which has been shown to both concentrate in the breast and to reduce breast cancer relapse in pre-menopausal women (Holliday et al, 2013; Shin et al, 2012; Wang et al, 2008; Formelli et al, 1993; Sabichi et al, 2003; Veronesi et al, 2006). ATRA (all-trans retinoic acid) is also a vitamin A analogue that is a highly effective therapeutic agent in acute promyelocitic leukemia patients.

Treatment of mammary tumor cells with clinically relevant concentrations of FTY720 (~50 nM) rapidly increased the levels of multiple dihydro-ceramide species (Figure S3J). At clinically relevant single agent concentrations that lacked individual toxicity, FTY720 or 4HPR significantly enhanced the lethality of [celecoxib + sildenafil] treatment in multiple tumor cell types (Figures S3K-S3M). Similar data to that with FTY720 or 4HPR were also observed using ATRA (Figure S3N).

FTY720 is known to act as an HDAC inhibitor, and prior studies from our group have demonstrated that multiple HDAC inhibitors can increase expression of CD95. In agreement with FTY720 being an HDAC inhibitor, the acetylation of histones in treated tumor cells was increased by the drug which was also associated with increased expression of CD95 (Figure S3O). Knock down of HDAC1 and HDAC2, the HDACI targets of FTY720, also increased CD95 expression, and knock down of CD95 or incubation of cells with fumonisin B1 suppressed killing by FTY720 + celecoxib + sildenafil treatment (Figure S3P). Similar data were obtained using 4HPR and ATRA (Figures S3Q and S3R).

Accepted Article

As noted for [celecoxib + sildenafil] treatment previously, treatment of cells with [celecoxib + sildenafil + FTY720] had a radiosensitizing effect (Figure S3S). Finally, based on prior and present knowledge that FTY720 increases ceramide levels and that 4HPR inhibits ceramide degradation we compared the ability of FTY720 and 4HPR treatment to enhance [celecoxib + sildenafil] toxicity. Combined treatment of tumor cells with FTY720 and 4HPR and with [celecoxib + sildenafil] resulted in profound levels of cell killing at times 9h after exposure (Figure S3T). Of note, both fumonisin B1 and myriocin prevented killing by [CEL / SIL / FTY] but myriocin only partially protected cells from [CEL / SIL / FTY / 4HPR] (Figure S3T).

We next determined whether our in vitro data with sildenafil and celecoxib and with [sildenafil + celecoxib] + FTY720 translated into animal model systems (Figure 6). In our first series of studies we injected 1 x 10^6 cells and pre-formed large mammary tumors in the fat pads of female athymic mice (~150 mm^3). Animals were treated for 6 days with either vehicle, sildenafil, celecoxib or both drugs simultaneously. Treatment of animals with celecoxib and sildenafil significantly reduced the growth of tumors below that of celecoxib alone (Figure 6A). In the second series of studies we injected 3 x 10^6 cells and 4 days after injection animals were treated for 7 days with either vehicle, sildenafil, celecoxib or both drugs simultaneously. Treatment of animals with celecoxib and sildenafil significantly reduced the formation and growth of tumors below that of celecoxib alone (Figure 6B). Similar data to that in Figure 6A were obtained using triple negative BC cells treated with drugs for 5 days (Figure 6C). We next injected 1 x 10^7 BT549 cells into the fat pad and 4 days after injection tumors of ~150 mm^3 had formed, and animals were treated with either vehicle, [sildenafil + celecoxib], FTY720 or all three drugs simultaneously. Treatment of animals with celecoxib and sildenafil and FTY720 significantly reduced the growth of tumors below that of celecoxib and sildenafil alone (Figure 6D). This was associated with increased animal survival (Figure 6E). Similar data to that in breast cancer was observed in GBM (Figure S3U). Of note, treatment of animals with higher doses of sildenafil and celecoxib and FTY720 above those used in tumor studies and for the same amount of time did not cause noticeable normal tissue toxicity as judged using H&E staining (Figure S4). Thus sildenafil and

Accepted Article

celecoxib treatment safely suppresses BC and GBM tumor growth in vivo which is enhanced by the FDA approved multiple sclerosis drug FTY720 (Fingolimod, Gilenya).

Discussion.

The present studies were performed to determine whether clinically relevant PDE5 inhibitors interacted with the COX2 inhibitor celecoxib to kill cancer cells. In multiple tumor cell types, including anoikis resistant and stem cell-like cells, sildenafil (and tadalafil) interacted with celecoxib to promote killing in short-term assays and long-term colony formation assays. Knock down of PDE5 recapitulated the combinatorial effect of a PDE5 inhibitor when combined with celecoxib. PDE5 inhibitors are known to enhance cGMP and NO levels; inhibition of NOS enzymes by L-NAME prevented the killing interaction between sildenafil and celecoxib. Our data also argued that celecoxib was acting in a COX2-independent manner when combined with sildenafil to promote cell death. Thus celecoxib, in a COX2 –independent fashion, promotes tumor cell killing in cells lacking PDE5 expression and does so in an NOS –dependent manner.

The molecular mechanisms by which sildenafil and celecoxib interact to kill were then investigated. Drug combination treatment tended to inactivate signaling pathways normally associated with cell survival (ERK, AKT, p70 S6K, mTOR, NFκB) and to activate pathways normally associated with cell killing (JNK, p38 MAPK). Based on the use of site specific RAS mutants and molecular tools we noted that combined signaling by ERK and AKT, or activation of mTOR, was required to prevent the synergy of drug interaction. Of note, others have argued that NO-induced DNA damage through ATM can suppress mTOR function (Tripathi et al, 2013). Inhibition of p38 MAPK and to a greater extent JNK blocked cell killing by the combination. As noted above, L-NAME prevented the killing interaction between sildenafil and celecoxib, and incubation of cells with the NOS inhibitor L-NAME blocked JNK activation.

Accepted Article

The cell death pathway(s) by which sildenafil and celecoxib interacted to kill were also determined. Inhibition of both the intrinsic and extrinsic apoptosis pathways reduced killing. The drug combination activated the death receptor CD95 in a tyrosine phosphorylation independent fashion and knock down of CD95 or FADD suppressed the toxic drug interaction. JNK activation, already shown to be a toxic signal, was CD95 dependent. And, activation of CD95 was suppressed by inhibition of NOS enzymes using L-NAME. Thus celecoxib and sildenafil in an NOS-dependent fashion activate CD95 which plays a key role in the activation of JNK which signals towards cell death. Studies by others have shown that nitrosylation of CD95 at its regulatory tyrosine residues inhibits CD95 signaling (Reinehr et al, 2004). Others however have argued that NO signaling and CD95 activation can cooperate to induce cell death (Gandelman et al, 2013; Gonzalez et al, 2013). The precise mechanism(s) by which NO signaling regulates CD95 function in our system in combination with celecoxib will require studies beyond the scope of the present manuscript.

In addition to activating the extrinsic apoptosis pathway, the drug combination also increased the numbers of autophagosomes and autolysosomes, i.e. "autophagy," in a time dependent fashion that was inhibited by incubation of the cells with L-NAME. Inhibition of autophagy suppressed cell killing. Nitric oxide signaling has been linked by others to the regulation of autophagy; in some primary non-transformed cells NO can inhibit autophagy by inhibiting JNK signaling (Shen et al, 2014; Benavides et al, 2013). In some transformed cells NO signaling can promote autophagy in an mTOR-dependent fashion which seems to play a role in tumor cell killing (Tripathi et al, 2013; Yu et al, 2012). We discovered that the drug combination inactivated mTOR, and expression of an activated form of mTOR suppressed killing, as well as autophagy as judged by GFP+ and RFP+ cells (unpublished data). The inactivation of mTOR was also blocked by incubation with L-NAME (unpublished data). Thus nitric oxide signaling plays a key role in both de-repressing a brake on toxic autophagy (mTOR) as well as promoting activation of the CD95/JNK apoptosis pathway.

Accepted Article

The regulation of CD95 activation has been proposed to require tyrosine phosphorylation of the receptor but also the generation of ceramide species (e.g. Cremesti et al, 2001). In prior studies by our group using different therapeutic drug combinations we have found that ceramide synthase 6 –mediated generation of ceramide played an important role in CD95 activation and tumor cell killing (e.g. Park et al, 2010). Celecoxib and sildenafil treatment increased the levels of [C16:0, C24:1, C24:0] dihydro-ceramide species; indicative that ceramide synthases 2, 3, and 6 were activated. Pan inhibition of ceramide synthase activity using fumonisin B1 suppressed the activation of CD95 and JNK, and enhanced levels of autophagy. Knock down of ceramide synthase 6 protected cells from drug combination toxicity. In smooth and cardiac muscle cells inhibition of ceramide synthase enzymes blocks nitric oxide toxicity (Pilane et al, 2004; Rabkin et al, 2002).

Recently, several studies have demonstrated that inhibitors of ceramide desaturase, the last enzyme in the de novo synthesis of ceramide, also elevate levels of dihydro-ceramide species and consequently induce cell killing and autophagy of diverse cancer cell lines i.e. the vitamin A analogue fenretinide (4HPR). And in addition, FTY720 is known to decrease sphingosine-1-phosphate signaling and to increase dihydro-ceramide levels. Our data demonstrated that either 4HPR, ATRA or FTY720 at clinically achievable concentrations could enhance the lethality of [celecoxib + sildenafil] treatment in vitro and in vivo. These findings suggest that the planned for clinical translation of the celecoxib and sildenafil concept should also possibly include a lagging arm of the trial in which the toxicity of a three drug combination with FTY720 (or ATRA) is determined. Unfortunately Novartis, the makers of Fingolimod, do not wish to support the oncologic translation of this drug due to its financial relevance to the company and the possible discovery of additional contraindications in cancer patients. As Fingolimod/Gilenya (standard of care, 0.5 mg / day per patient) costs ~$7,500 / month, it is highly unlikely that our three drug combination approach will reach the clinical arena in the foreseeable future. Additional studies will also be required to determine whether

Accepted Article

ceramide synthase and desaturase enzyme activities are regulated by protein nitration or by celecoxib – induced ER stress signaling.

Celecoxib levels in human plasma and tissues after a 200-800 mg single dose can reach up to ~2.5-7.5 μM and it is evident that the drug at these concentrations has chemo-preventative effects in patients. Although the majority of celecoxib is albumin bound in plasma after a 200-800 mg single dose, the partitioning of celecoxib into multiple organs occurs rapidly and after 5 days of dosing the levels of celecoxib in the plasma and in tissues reach equilibrium at ~5-10 μM. This delivery and partitioning process is similar in concept to the delivery of paclitaxel using albumin as a carrier (i.e. Abraxane). As celecoxib has been safely dosed on a daily basis at up to 2,600 mg QD for two weeks our in vitro studies using 5 μM celecoxib will be well within the physiologically achievable range of free drug in a human tumor. Sildenafil has been safely administered to patients at doses of up to 200 mg, with peak plasma levels in the ~3 μM range and a bioavailability of ~40% (Nichols et al, 2002). Our data in Figure 1 would argue that at sildenafil concentrations as low as 0.5 μM we can observe a significant interaction with celecoxib, again suggesting that we are within the physiologically achievable range of free drug. Similarly, using clinically achievable concentrations of 4HPR (200 nM), ATRA (150 nM) and FTY720 (50 nM) we were able to demonstrate drug interactions in vitro and in vivo. As FTY720 is known to concentrate in the brain (and lung and adipose tissue) our data strongly argue that the clinical translation of [celecoxib + sildenafil + FTY720] in mammary tissue in situ, NSCLC and GBM should be explored.

Celecoxib at much higher concentrations than used in the present studies has been reported to cause ER stress signaling (Chen et al, 2010; Kardosh et al, 2008; Tsutsumi et al, 2004). We noted that whilst celecoxib as a single agent at 5 μM did not strongly increase eIF2α phosphorylation the drug combination did increase the phosphorylation of eIF2α, and we then interrogated the three arms of the ER stress response

Accepted Article

as to whether they controlled the level of cell killing. Inhibition of the IRE1α/XBP1 arm of the stress response enhanced both celecoxib and (celecoxib + sildenafil) lethality whereas inhibition of the eIF2α/ATF4/CHOP arm of the response protected cells. Celecoxib at 10-fold higher levels, through an eIF2α/ATF4/CHOP pathway, has been proposed to increase expression of the death receptor DR5 (Oh et al, 2010). Others have shown celecoxib to increase CD95 levels (Kern et al, 2006). Thus it is probable that our observed activation of death receptor signaling may be augmented in the long term by signaling by newly synthesized death receptors. Additional studies beyond the scope of this manuscript will be required to identify the proteins downstream of the IRE1α/XBP1 arm of the ER stress response that control the apoptotic threshold.

In conclusion, we have discovered that the approved NSAID celecoxib can interact with approved PDE5 inhibitors to kill a wide range of tumor cell types at physiologically relevant concentrations. In some Westerner European nations it has frequently been difficult for cancer patients to obtain the latest most expensive standard of care therapeutics drugs due to Governmental committee decisions e.g. as previously reported for Velcade, Sorafenib, Abiraterone. The studies in this manuscript, particularly those combining the generic drugs Celebrex, Viagra and ATRA could thus become a cost-effective approach to treat cancer patients with a wide variety of solid malignancies in countries with limited financial resources. Based on the studies presented in this manuscript it is hoped that clinical translation of the two drug [celecoxib + sildenafil] combination will occur in the near future.

Accepted Article

References

Bastos-Pereira AL, Lugarini D, Oliveira-Christoff Ad, Ávila TV, Teixeira S, Pires Ado R, Muscará MN, Cadena SM, Donatti L, Cristina da Silva de Assis H, Acco A. Celecoxib prevents tumor growth in an animal model by a COX-2 independent mechanism. Cancer Chemother Pharmacol. 2010;65:267-76.

Benavides GA, Liang Q, Dodson M, Darley-Usmar V, Zhang J. Inhibition of autophagy and glycolysis by nitric oxide during hypoxia-reoxygenation impairs cellular bioenergetics and promotes cell death in primary neurons. Free Radic Biol Med. 2013;65:1215-28.

Bruzziches R, Francomano D, Gareri P, Lenzi A, Aversa A. An update on pharmacological treatment of erectile dysfunction with phosphodiesterase type 5 inhibitors. Expert Opin Pharmacother. 2013;14:1333-44.

Booth L, Cazanave SC, Hamed HA, Yacoub A, Ogretmen B, Chen CS, Grant S, Dent P. OSU-03012 suppresses GRP78/BiP expression that causes PERK-dependent increases in tumor cell killing. Cancer Biol Ther. 2012; 13:224-36.

Booth L, Roberts JL, Cruickshanks N, Conley A, Durrant DE, Das A, Fisher PB, Kukreja RC, Grant S, Poklepovic A, Dent P. Phosphodiesterase 5 inhibitors enhance chemotherapy killing in gastrointestinal / genitourinary cancer cells. Mol Pharmacol. 2014;85:408-19.

Carón RW, Yacoub A, Li M, Zhu X, Mitchell C, Hong Y, Hawkins W, Sasazuki T, Shirasawa S, Kozikowski AP, Dennis PA, Hagan MP, Grant S, Dent P. Activated forms of H-RAS and K-RAS differentially regulate membrane association of PI3K, PDK-1, and AKT and the effect of therapeutic kinase inhibitors on cell survival. Mol Cancer Ther. 2005;4:257-70.

Accepted Article

Chandrasekharan NV, Dai H, Roos KL, Evanson NK, Tomsik J, Elton TS, Simmons DL. COX-3, a cyclooxygenase-1 variant inhibited by acetaminophen and other analgesic/antipyretic drugs: Cloning, structure, and expression. Proc. Natl. Acad. Sci. U.S.A. 2002; 99: 13926–31.

Chen ST, Thomas S, Gaffney KJ, Louie SG, Petasis NA, Schönthal AH. Cytotoxic effects of celecoxib on Raji lymphoma cells correlate with aggravated endoplasmic reticulum stress but not with inhibition of cyclooxygenase-2. Leuk Res. 2010;34:250-3.

Chen S, Cao W, Yue P, Hao C, Khuri FR, Sun SY. Celecoxib promotes c-FLIP degradation through Akt-independent inhibition of GSK3. Cancer Res. 2011;71:6270-81.

Choi DE, Jeong JY, Lim BJ, Chung S, Chang YK, Lee SJ, Na KR, Kim SY, Shin YT, Lee KW. Pretreatment of sildenafil attenuates ischemia-reperfusion renal injury in rats. Am J Physiol Renal Physiol. 2009; 297:F362-70.

Chuang HC, Kardosh A, Gaffney KJ, Petasis NA, Schönthal AH. COX-2 inhibition is neither necessary nor sufficient for celecoxib to suppress tumor cell proliferation and focus formation in vitro. Mol Cancer. 2008;7:38.

Cremesti A, Paris F, Grassmé H, Holler N, Tschopp J, Fuks Z, Gulbins E, Kolesnick R. Ceramide enables fas to cap and kill. J Biol Chem. 2001;276:23954-61.

Cruickshanks N, Hamed HA, Booth L, Tavallai S, Syed J, Sajithlal GB, Grant S, Poklepovic A, Dent P. Histone deacetylase inhibitors restore toxic BH3 domain protein expression in anoikis-resistant mammary and brain cancer stem cells, thereby enhancing the response to anti-ERBB1/ERBB2 therapy. Cancer Biol Ther. 2013;14:982-96.

Accepted Article

Das A, Durrant D, Mitchell C, Mayton E, Hoke NN, Salloum FN, Park MA, Qureshi I, Lee R, Dent P, Kukreja RC. Sildenafil increases chemotherapeutic efficacy of doxorubicin in prostate cancer and ameliorates cardiac dysfunction. Proc Natl Acad Sci U S A. 2010;107:18202-7.

Das A, Xi L, Kukreja RC. Protein kinase G-dependent cardioprotective mechanism of phosphodiesterase-5 inhibition involves phosphorylation of ERK and GSK3beta. J Biol Chem. 2008;283:29572-85.

Eberle A, Reinehr R, Becker S, Keitel V, Häussinger D. CD95 tyrosine phosphorylation is required for CD95 oligomerization. Apoptosis. 2007;12:719-29.

Florio T, Arena S, Pattarozzi A, Thellung S, Corsaro A, Villa V, Massa A, Diana F, Spoto G, Forcella S, Damonte G, Filocamo M, Benatti U, Schettini G. Basic fibroblast growth factor activates endothelial nitric-oxide synthase in CHO-K1 cells via the activation of ceramide synthesis. Mol Pharmacol. 2003;63:297-310.

Flower RJ. The development of COX2 inhibitors. Nat Rev Drug Discov. 2003;2:179-91.

Formelli F, Clerici M, Campa T, Di Mauro M, Magni A, Mascotti G, Moglia D, De Palo G, Costa A, Veronesi U. Five-Year Administration of Fenretinide: Pharmacokinetics and Effects on Plasma Retinol Concentrations. J. Clin. Oncol. 1993: 11; 2036–2042.

Francis SH, Busch JL, Corbin JD, Sibley D. cGMP-dependent protein kinases and cGMP phosphodiesterases in nitric oxide and cGMP action. Pharmacol Rev. 2010;62:525-63.

Gandelman M, Levy M, Cassina P, Barbeito L, Beckman JS. P2X7 receptor-induced death of motor neurons by a peroxynitrite/FAS-dependent pathway. J Neurochem. 2013;126:382-8.

Accepted Article

Giannini C, Sarkaria JN, Saito A, Uhm JH, Galanis E, Carlson BL, Schroeder MA, James CD. Patient tumor EGFR and PDGFRA gene amplifications retained in an invasive intracranial xenograft model of glioblastoma multiforme. Neuro Oncol. 2005;7:164-76.

González R, Ferrín G, Aguilar-Melero P, Ranchal I, Linares CI, Bello RI, De la Mata M, Gogvadze V, Bárcena JA, Alamo JM, Orrenius S, Padillo FJ, Zhivotovsky B, Muntané J. Targeting hepatoma using nitric oxide donor strategies. Antioxid Redox Signal. 2013;18:491-506.

Grösch S, Tegeder I, Niederberger E, Bräutigam L, Geisslinger G. COX-2 independent induction of cell cycle arrest and apoptosis in colon cancer cells by the selective COX-2 inhibitor celecoxib. FASEB J. 2001;15:2742-4.

Hamed HA, Yamaguchi Y, Fisher PB, Grant S, Dent P. Sorafenib and HDAC inhibitors synergize with TRAIL to kill tumor cells. J Cell Physiol. 2013;228:1996-2005.

Hayden MA, Lange PA, Nakayama DK. Nitric oxide and cyclic guanosine monophosphate stimulate apoptosis via activation of the Fas-FasL pathway. J Surg Res. 2001;101:183-9.

Holliday MW Jr, Cox SB, Kang MH, Maurer BJ. C22:0- and C24:0-dihydroceramides confer mixed cytotoxicity in T-cell acute lymphoblastic leukemia cell lines. PLoS One. 2013; 8:e74768.

Hsieh PS, Tsai HC, Kuo CH, Chan JY, Shyu JF, Cheng WT, Liu TT. Selective COX2 inhibition improves whole body and muscular insulin resistance in fructose-fed rats. Eur J Clin Invest. 2008;38:812-9.

Accepted Article

Hsu AL, Ching TT, Wang DS, Song X, Rangnekar VM, Chen CS. The cyclooxygenase-2 inhibitor celecoxib induces apoptosis by blocking Akt activation in human prostate cancer cells independently of Bcl-2. J Biol Chem. 2000;275:11397-403.

Huang KH, Kuo KL, Ho IL, Chang HC, Chuang YT, Lin WC, Lee PY, Chang SC, Chiang CK, Pu YS, Chou CT, Hsu CH, Liu SH. Celecoxib-induced cytotoxic effect is potentiated by inhibition of autophagy in human urothelial carcinoma cells. PLoS One. 2013;8:e82034.

Johnson AJ, Song X, Hsu A, Chen C. Apoptosis signaling pathways mediated by cyclooxygenase-2 inhibitors in prostate cancer cells. Adv Enzyme Regul. 2001;41:221-35.

Kardosh A, Golden EB, Pyrko P, Uddin J, Hofman FM, Chen TC, Louie SG, Petasis NA, Schönthal AH. Aggravated endoplasmic reticulum stress as a basis for enhanced glioblastoma cell killing by bortezomib in combination with celecoxib or its non-coxib analogue, 2,5-dimethyl-celecoxib. Cancer Res. 2008;68:843-51.

Kern MA, Haugg AM, Koch AF, Schilling T, Breuhahn K, Walczak H, Fleischer B, Trautwein C, Michalski C, Schulze-Bergkamen H, Friess H, Stremmel W, Krammer PH, Schirmacher P, Müller M. Cyclooxygenase-2 inhibition induces apoptosis signaling via death receptors and mitochondria in hepatocellular carcinoma. Cancer Res. 2006;66:7059-66.

Kim B, Giardiello FM. Chemoprevention in familial adenomatous polyposis. Best Pract Res Clin Gastroenterol. 2011;25:607-22.

Accepted Article

Komalavilas P, Shah PK, Jo H, Lincoln TM. Activation of mitogen-activated protein kinase pathways by cyclic GMP and cyclic GMP-dependent protein kinase in contractile vascular smooth muscle cells. J Biol Chem. 1999;274:34301-9.

Kots AY, Bian K, Murad F. Nitric oxide and cyclic GMP signaling pathway as a focus for drug development. Curr Med Chem. 2011;18:3299-305.

Liu X, Yue P, Zhou Z, Khuri FR, Sun SY. Death receptor regulation and celecoxib-induced apoptosis in human lung cancer cells. J Natl Cancer Inst. 2004;96:1769-80.

Mao JT, Roth MD, Fishbein MC, Aberle DR, Zhang ZF, Rao JY, Tashkin DP, Goodglick L, Holmes EC, Cameron RB, Dubinett SM, Elashoff R, Szabo E, Elashoff D. Lung cancer chemoprevention with celecoxib in former smokers. Cancer Prev Res (Phila). 2011;4:984-93.

Nandakishore R, Ravikiran Y, Rajapranathi M. Selective Cyclooxygenase Inhibitors: Current Status. Curr Drug Discov Technol. 2014 Jan 27. [Epub ahead of print]

Nichols DJ, Muirhead GJ, Harness JA. Pharmacokinetics of sildenafil after single oral doses in healthy male subjects: absolute bioavailability, food effects and dose proportionality. Br. J. Clin. Pharmacol. 2002; 53(S1): 5S-12S.

Oh YT, Liu X, Yue P, Kang S, Chen J, Taunton J, Khuri FR, Sun SY. ERK/ribosomal S6 kinase (RSK) signaling positively regulates death receptor 5 expression through co-activation of CHOP and Elk1. J Biol Chem. 2010;285:41310-9.

Accepted Article

Park MA, Yacoub A, Rahmani M, Zhang G, Hart L, Hagan MP, Calderwood SK, Sherman MY, Koumenis C, Spiegel S, Chen CS, Graf M, Curiel DT, Fisher PB, Grant S, Dent P. OSU-03012 stimulates PKR-like endoplasmic reticulum-dependent increases in 70-kDa heat shock protein expression, attenuating its lethal actions in transformed cells. Mol Pharmacol. 2008; 73: 1168-84.

Park MA, Mitchell C, Zhang G, Yacoub A, Allegood J, Häussinger D, Reinehr R, Larner A, Spiegel S, Fisher PB, Voelkel-Johnson C, Ogretmen B, Grant S, Dent P. Vorinostat and sorafenib increase CD95 activation in gastrointestinal tumor cells through a Ca(2+)-de novo ceramide-PP2A-reactive oxygen species-dependent signaling pathway. Cancer Res. 2010;70:6313-24.

Pilane CM, LaBelle EF. NO induced apoptosis of vascular smooth muscle cells accompanied by ceramide increase. J Cell Physiol. 2004;199:310-5.

Piplani H, Rana C, Vaish V, Vaiphei K, Sanyal SN. Dolastatin, along with Celecoxib, stimulates apoptosis by a mechanism involving oxidative stress, membrane potential change and PI3-K/AKT pathway down regulation. Biochim Biophys Acta. 2013;1830:5142-56.

Pyrko P, Kardosh A, Liu YT, Soriano N, Xiong W, et al. Calcium-activated endoplasmic reticulum stress as a major component of tumor cell death induced by 2,5-dimethyl-celecoxib, a non-coxib analogue of celecoxib. Mol Cancer Ther 2007;6: 1262-1275.

Rabkin SW. Fumonisin blunts nitric oxide-induced and nitroprusside-induced cardiomyocyte death. Nitric Oxide. 2002;7:229-35.

Ramer R, Walther U, Borchert P, Laufer S, Linnebacher M, Hinz B. Induction but not inhibition of COX-2 confers human lung cancer cell apoptosis by celecoxib. J Lipid Res. 2013;54:3116-29.

Accepted Article

Reinehr R, Görg B, Höngen A, Häussinger D. CD95-tyrosine nitration inhibits hyperosmotic and CD95 ligand-induced CD95 activation in rat hepatocytes. J Biol Chem. 2004;279:10364-73.

Roberts JL, Conley A, Booth L, Cruickshanks N, Malkin M, Kukreja RC, Grant S, Poklepovic A, Dent P. PDE5 inhibitors enhance the lethality of standard of care chemotherapy in pediatric CNS tumor cells. Cancer Biol. Ther. (2014). IN PRESS.

Russwurm M, Russwurm C, Koesling D, Mergia E. NO/cGMP: the past, the present, and the future. Methods Mol Biol. 2013;1020:1-16.

Saba N, Hurwitz SJ, Kono S, Yang CS, Zhao Y, Chen Z, Sica GL, Muller S, Moreno-Williams R, Lewis M, Grist W, Chen AY, Moore CE, Owonikoko TK, Ramalingam SS, Beitler JJ, Nannapaneni S, Shin HJ, Grandis JR, Khuri FR, Chen ZG, Shin DM. Chemoprevention of Head and Neck Cancer with Celecoxib and Erlotinib: Results of a Phase 1b and Pharmacokinetic Study. Cancer Prev Res (Phila). 2013 Oct 3. [Epub ahead of print]

Sabichi A, Modiano M, Lee JJ, Peng YM, Xu MJ, Vallar H, Dalton W, Lippman S. Breast Tissue Accumulation of Retinamides in a Randomized Short-term Study of Fenretinide. Clin Cancer Res. 2003: 9; 2400–2405.

Schiffmann S, Ziebell S, Sandner J, Birod K, Deckmann K, Hartmann D, Rode S, Schmidt H, Angioni C, Geisslinger G, Grösch S. Activation of ceramide synthase 6 by celecoxib leads to a selective induction of C16:0-ceramide. Biochem Pharmacol. 2010;80:1632-40.

Schiffmann S, Maier TJ, Wobst I, Janssen A, Corban-Wilhelm H, Angioni C, Geisslinger G, Grösch S. The anti-proliferative potency of celecoxib is not a class effect of coxibs. Biochem Pharmacol. 2008;76:179-87.

Accepted Article

Shen C, Yan J, Erkocak OF, Zheng XF, Chen XD. Nitric oxide inhibits autophagy via suppression of JNK in meniscal cells. Rheumatology (Oxford). 2014 Feb 5. [Epub ahead of print].

Shin KO1, Park NY, Seo CH, Hong SP, Oh KW, Hong JT, Han SK, Lee YM. Inhibition of sphingolipid metabolism enhances resveratrol chemotherapy in human gastric cancer cells. Biomol Ther (Seoul). 2012; 20: 470-6.

Soh JW, Kazi JU, Li H, Thompson WJ, Weinstein IB. Celecoxib-induced growth inhibition in SW480 colon cancer cells is associated with activation of protein kinase G. Mol Carcinog. 2008;47:519-25.

Song J, Chen Q, Xing D. Enhanced apoptotic effects by downregulating Mcl-1: evidence for the improvement of photodynamic therapy with Celecoxib. Exp Cell Res. 2013;319:1491-504.

Swiergiel AH, Dunn AJ. Distinct roles for cyclooxygenases 1 and 2 in interleukin-1-induced behavioral changes. J Pharmacol Exp Ther. 2002;302:1031-6.

Tang Y, Hamed HA, Cruickshanks N, Fisher PB, Grant S, Dent P. Obatoclax and lapatinib interact to induce toxic autophagy through NOXA. Mol Pharmacol. 2012;81:527-40.

Tripathi DN, Chowdhury R, Trudel LJ, Tee AR, Slack RS, Walker CL, Wogan GN. Reactive nitrogen species regulate autophagy through ATM-AMPK-TSC2-mediated suppression of mTORC1. Proc Natl Acad Sci U S A. 2013;110:E2950-7.

Accepted Article

Tsutsumi S, Gotoh T, Tomisato W, Mima S, Hoshino T, Hwang HJ, Takenaka H, Tsuchiya T, Mori M, Mizushima T. Endoplasmic reticulum stress response is involved in nonsteroidal anti-inflammatory drug-induced apoptosis. Cell Death Differ. 2004;11:1009-16.

Veronesi U.; Mariani L, Decensi A, Formelli F, Camerini T, Miceli R, Di Mauro MG, Costa A, Marubini E, De Palo MB. Fifteen-year results of a randomized phase III trial of fenretinide to prevent second breast cancer. 2006: 17; 1065–1071.

Vosooghi M, Amini M. The discovery and development of cyclooxygenase-2 inhibitors as potential anticancer therapies. Expert Opin Drug Discov. 2014 Feb 3. [Epub ahead of print]

Wang H, Maurer BJ, Liu YY, Wang E, Allegood JC, Kelly S, Symolon H, Liu Y, Merrill AH Jr, Gouazé-Andersson V, Yu JY, Giuliano AE, Cabot MC. N-(4-Hydroxyphenyl)retinamide increases dihydroceramide and synergizes with dimethylsphingosine to enhance cancer cell killing. Mol Cancer Ther. 2008;7:2967-76.

Watanabe H, Ohashi K, Takeuchi K, Yamashita K, Yokoyama T, Tran QK, Satoh H, Terada H, Ohashi H, Hayashi H. Sildenafil for primary and secondary pulmonary hypertension. Clin Pharmacol Ther. 2002;71:398-402.

Werner U, Werner D, Pahl A, Mundkowski R, Gillich M, Brune K. Investigation of the pharmacokinetics of celecoxib by liquid chromatography-mass spectrometry. Biomed Chromatogr. 2002;16:56-60.

Accepted Article

Williams CS, Watson AJ, Sheng H, Helou R, Shao J, DuBois RN. Celecoxib prevents tumor growth in vivo without toxicity to normal gut: lack of correlation between in vitro and in vivo models. Cancer Res. 2000;60:6045-51.

Yacoub A, Park MA, Hanna D, Hong Y, Mitchell C, Pandya AP, Harada H, Powis G, Chen CS, Koumenis C, Grant S, Dent P. OSU-03012 promotes caspase-independent but PERK-, cathepsin B-, BID-, and AIF-dependent killing of transformed cells. Mol Pharmacol. 2006; 70:589-603.

Yu Y, Fan SM, Yuan SJ, Tashiro S, Onodera S, Ikejima T. Nitric oxide (•NO) generation but not ROS plays a major role in silibinin-induced autophagic and apoptotic death in human epidermoid carcinoma A431 cells. Free Radic Res. 2012;46:1346-60.

Accepted Article

Footnotes

Support for the present study was funded from PHS grants from the National Institutes of Health [R01-CA141704, R01-CA150214, R01-DK52825, R01-CA61774]. Thanks to Mrs. Grizzard for her support to the Dent lab and to the Betts family fund for support in the purchase of the Hermes Wiscan instrument. Thanks to the VCU TDAAC, Dr. G. Tye and Dr. W.C. Broaddus in the procurement and rapid delivery of fresh tumor tissue from the OR. We gratefully acknowledge the essential assistance of the VCU lipidomics / Metabolomics core in performing our ceramide and S1P analyses, which is supported in part by funding from the NIH-NCI Massey Cancer Center support grant CA016059. We acknowledge that the basic histology of normal tissue sections was performed at the VCU Massey Cancer Center Macromolecule Core Facility sponsored in part with funding from NCI Cancer Core Grant P30 CA016059. PD is the holder of the Universal Inc. Chair in Signal Transduction Research. The authors have no conflicts of interest to report. This manuscript is black and white but red all over and is dedicated to the memory of Crazy Horse and Wor Jackie.

Accepted Article

Figure Legends

Figure 1. The PDE5 inhibitor sildenafil interacts with celecoxib to kill cancer cell lines. (A) SKBR3 and BT549 cells were treated with celecoxib (5 μM) and increasing concentrations of sildenafil (0-2 μM). SKBR3 and BT549 cells were treated with sildenafil (2 μM) and increasing concentrations of celecoxib (0-5 μM).Cells were isolated after 24h and viability determined by trypan blue exclusion (n = 3, +/- SEM) * $p < 0.05$ greater than corresponding value in vehicle control. **(B)** Breast cancer cells, wild type (WT) or anoikis resistant (AR) variants, were treated with celecoxib (CEL 5.0 μM) and/or sildenafil (SIL, 2.0 μM). Cells were isolated after 24h and viability determined by trypan blue exclusion (n = 3, +/- SEM) * $p < 0.05$ greater than corresponding value in vehicle control. Upper inset pictures: BT474 cells in 96 well plates were treated with celecoxib (CEL 5.0 μM) and/or sildenafil (SIL, 2.0 μM). Cells were isolated after 24h and viability determined using a live-dead assay (red cells = dead; green cells = alive) (n = 3, +/- SEM) * $p < 0.05$ greater than corresponding value in vehicle control. **(C)** Breast cancer cells, wild type (WT) or anoikis resistant (AR) variants, were treated with celecoxib (CEL 5.0 μM) and/or sildenafil (SIL, 2.0 μM). Cells were isolated after 24h and viability determined by trypan blue exclusion (n = 3, +/- SEM) * $p < 0.05$ greater than corresponding value in vehicle control. Upper inset pictures: HCC38 cells in 96 well plates were treated with celecoxib (CEL 5.0 μM) and/or sildenafil (SIL, 2.0 μM). Cells were isolated after 24h and viability determined using a live-dead assay (red cells = dead; green cells = alive) (n = 3, +/- SEM) * $p < 0.05$ greater than corresponding value in vehicle control. **(D)** GBM12 cells and selected GBM12 stem cells were treated with celecoxib (CEL 5.0 μM) and/or sildenafil (SIL, 2.0 μM). Cells were isolated after 24h and viability determined by trypan blue exclusion (n = 3, +/- SEM) * $p < 0.05$ greater than corresponding value in vehicle control. Upper inset pictures GBM12 cells in 96 well plates were treated with celecoxib (CEL 5.0 μM) and/or sildenafil (SIL, 2.0 μM). Cells were isolated after 24h and viability determined using a live-dead assay (red cells = dead; green cells = alive) (n = 3, +/- SEM) * $p < 0.05$ greater than corresponding value in vehicle control. **(E)** Medulloblastoma cells were treated with celecoxib (CEL 5.0 μM) and/or sildenafil (SIL, 2.0 μM). Cells were isolated after 24h and viability determined by trypan blue

Accepted Article

exclusion (n = 3, +/- SEM) * $p < 0.05$ greater than corresponding value in vehicle control. Upper inset pictures: DAOY medulloblastoma cells in 96 well plates were treated with celecoxib (CEL 5.0 μM) and/or sildenafil (SIL, 2.0 μM). Cells were isolated after 24h and viability determined using a live-dead assay (red cells = dead; green cells = alive) (n = 3, +/- SEM) * $p < 0.05$ greater than corresponding value in vehicle control. **(F)** *Upper IHC:* BT549 cells in 96 well plates were treated with celecoxib (CEL 5.0 μM) and/or sildenafil (SIL, 2.0 μM). Cells were isolated after 24h and fixed. Immunohistochemistry was performed to determine the levels of Ki67 staining in cells under each treatment condition. *Lower graphs:* BT549 triple negative breast and SUM149 triple negative inflammatory breast cancer cells were plated as single cells in sextuplicate (250-1500 cells per plate) and treated with vehicle (DMSO), sildenafil (1-3 μM), celecoxib (5 μM) or the drugs in combination as indicated for 24h. The media was removed and drug free media added to the cultures. Colonies were permitted to form for 10 days after which colonies were stained and counted (n = 3 +/- SEM). **(G)-(I)** Tumor cells (as indicated) were treated with sildenafil (2 μM); celecoxib (5 μM); FTY720 (50 nM) or ATRA (150 nM). One, two and 6h after treatment cells, as indicated, were fixed in place and permeabilized. Immunohistochemistry was performed to determine the levels of Phospho-VASP-1 (S239); Phospho-eIF2α; total EDG-1, and counter staining was with DAPI.

Accepted Article

Figure 2. PDE5 inhibitors enhance celecoxib toxicity. (A) DAOY and HOSS1 medulloblastoma cells were treated with celecoxib (CEL 5.0 μM) and/or tadalafil (TAD, 0.5 μM). Cells were isolated after 24h and viability determined by trypan blue exclusion (n = 3, +/- SEM) * $p < 0.05$ greater than corresponding value in vehicle control. **(B)** SKBR3 and BT474 breast cancer cells were treated with celecoxib (CEL 5.0 μM) and/or tadalafil (TAD, 0.5 μM). Cells were isolated after 24h and viability determined by trypan blue exclusion (n = 3, +/- SEM) * $p < 0.05$ greater than corresponding value in vehicle control. **(C) – (E)** We purchased tissue arrays of mammary / lung / liver carcinoma and matching normal tissues. Tissue was de-parafinized, blocked, and stained for expression of PDE5. The data shows representative images of matched normal and tumor tissue. **(F)** Tumor cells were treated with 2,5 dimethyl celecoxib (25DMC 5.0 μM) and/or sildenafil (SIL, 2.0 μM). Cells were isolated after 24h and viability determined by trypan blue exclusion (n = 3, +/- SEM) * $p < 0.05$ greater than corresponding value in vehicle control. **(G)** SUM149 cells were transfected with a scrambled siRNA (siSCR) or an siRNA to knock down COX2. Thirty six h after transfection cells were treated with celecoxib (CEL 5.0 μM) and/or sildenafil (SIL, 2.0 μM). Cells were isolated after 24h and viability determined by trypan blue exclusion (n = 3, +/- SEM) * $p < 0.05$ greater than corresponding value in vehicle control. **(H)** BT549 cells were transfected with a scrambled siRNA (siSCR) or an siRNA to knock down PDE5. Thirty six h after transfection cells were treated with increasing concentrations of celecoxib (0-7.5 μM). Cells were isolated after 24h and viability determined by trypan blue exclusion (n = 3, +/- SEM) * $p < 0.05$ greater than corresponding value in siSCR control. **(I)** and **(J)** BT549, BT474 breast and HOSS1 medulloblastoma cells were pre-treated with vehicle or the NOS inhibitor L-NAME (1 μM). After 30 min cells were treated with celecoxib (CEL 5.0 μM) and/or sildenafil (SIL, 2.0 μM). Cells were isolated after 24h and viability determined by trypan blue exclusion (n = 3, +/- SEM) * $p < 0.05$ greater than vehicle control; # $p < 0.05$ less than corresponding value in vehicle control. **(K)** BT474 and BT549 cells were plated as single cells in sextuplicate. Twelve h after plating cells were treated with vehicle (DMSO), celecoxib (2 μM), sildenafil (1 μM) or the drugs in combination as indicated. Thirty min after drug treatment cells were irradiated (2 Gy) or mock exposed (time out of incubator ~20 min).

Accepted Article

The media was replaced after 12h with drug free media and colonies permitted to form over the following 10 days. Colonies were fixed, stained and counted (n = 3 +/- SEM). # $p < 0.05$ less than corresponding value in unirradiated cells.

Accepted Article

Figure 3. The toxic interaction between PDE5 inhibitors and celecoxib is regulated by ERK, AKT, p70 S6K, p38 MAPK and mTOR. (A) BT549 cells were treated with celecoxib (CEL 5.0 μM) and/or sildenafil (SIL, 2.0 μM). Cells were isolated after 12h and lysates prepared for SDS PAGE and immunoblotting against the indicated phospho-proteins and proteins. **(B)** HCT116 colon cancer cells (Wild type cells expressing K-RAS D13; null -/- cells with K-RAS D13 deleted; null cells expressing H-RAS V12; null cells expressing H-RAS V12-35 that activates RAF-1; null cells expressing H-RAS V12-40 that activates PI3K) were treated with vehicle (DMSO), celecoxib (5.0 μM), sildenafil (2 μM) or the drugs combined. Twenty four h after drug treatment cells were isolated and viability determined by trypan blue exclusion assay (n = 3 +/- SEM). * $p < 0.05$ greater than vehicle control; ** $p < 0.05$ greater than corresponding value in HCT116 -/- H-RAS V12 cells. **(C)** BT549 cells were infected with recombinant adenoviruses to express empty vector (CMV); constitutively active AKT; dominant negative AKT (50 moi). Twenty four h after infection cells were treated with celecoxib (CEL 5.0 μM) and/or sildenafil (SIL, 2.0 μM). Twenty four h after drug treatment cells were isolated and viability determined by trypan blue exclusion assay (n = 3 +/- SEM). * $p < 0.05$ greater than corresponding value in CMV infected cells; # $p < 0.05$ less than corresponding value in CMV infected cells. **(D)** BT549 cells were infected with recombinant adenoviruses to express empty vector (CMV); constitutively active MEK1; dominant negative MEK1 (50 moi). Twenty four h after infection cells were treated with celecoxib (CEL 5.0 μM) and/or sildenafil (SIL, 2.0 μM). Twenty four h after drug treatment cells were isolated and viability determined by trypan blue exclusion assay (n = 3 +/- SEM). * $p < 0.05$ greater than corresponding value in CMV infected cells; # $p < 0.05$ less than corresponding value in CMV infected cells. **(E)** BT549 cells were transfected with plasmids to express empty vector (CMV); constitutively active p70 S6K; constitutively active mTOR; dominant negative p38. Twenty four h after transfection cells were treated with celecoxib (CEL 5.0 μM) and/or sildenafil (SIL, 2.0 μM). Twenty four h after drug treatment cells were isolated and viability determined by trypan blue exclusion assay (n = 3 +/- SEM). * $p < 0.05$ greater than corresponding value in CMV transfected cells; # $p < 0.05$ less than corresponding value in CMV transfected cells. **(F)** BT549 and

Accepted Article

HOSS1 cells were pre-treated with vehicle (DMSO) or the JNK inhibitory peptide (JNK-IP, 10 μM). Cells were then treated with celecoxib (CEL 5.0 μM) and/or sildenafil (SIL, 2.0 μM). Twenty four h after drug treatment cells were isolated and viability determined by trypan blue exclusion assay (n = 3 +/- SEM). * $p < 0.05$ greater than celecoxib treatment alone; # $p < 0.05$ less than corresponding value in vehicle treated cells. **(G)** GBM5/6/12/14 cells as indicated pre-treated with vehicle or the NOS inhibitor L-NAME (1 μM). After 30 min cells were treated with celecoxib (CEL 5.0 μM) and/or sildenafil (SIL, 2.0 μM). Cells were isolated after 12h and the phosphorylation of JNK and total JNK expression determined.

Accepted Article

Figure 4. Celecoxib and sildenafil –induced lethality is suppressed by inhibition of the intrinsic and extrinsic apoptosis pathways. (A) and **(B)** BT549, HOSS1 and DAOY cells were infected with recombinant adenoviruses to express empty vector (CMV); dominant negative caspase 9; BCL-XL; or c-FLIP-s. Twenty four h after infection cells were then treated with celecoxib (CEL 5.0 μM) and/or sildenafil (SIL, 2.0 μM). Twenty four h after drug treatment cells were isolated and viability determined by trypan blue exclusion assay (n = 3 +/- SEM). # $p < 0.05$ less than corresponding value in CMV infected cells. **(C)** BT549 and HOSS1 cells were transfected with a scrambled control siRNA (siSCR) or siRNA molecules to knock down expression of CD95 (siCD95) or FADD (siFADD). Thirty six h after transfection cells were then treated with celecoxib (CEL 5.0 μM) and/or sildenafil (SIL, 2.0 μM). Twenty four h after drug treatment cells were isolated and viability determined by trypan blue exclusion assay (n = 3 +/- SEM). # $p < 0.05$ less than corresponding value in siSCR transfected cells. **(D)** BT549 and HOSS1 cells in 96 well plates were treated with celecoxib (CEL 5.0 μM) and/or sildenafil (SIL, 2.0 μM). Six h after treatment cells were fixed to the plate and immunohistochemistry performed to determine the plasma membrane levels of CD95. The upper images obtained using the Hermes Wiscan imaging system is representative of the data. The intensity of CD95 immunostaining was determined using the Wisoft data analysis package (n = 3 +/- SEM). * $p < 0.05$ value greater than celecoxib treatment alone. **(E) and (F)** BT474 and BT549 cells were transfected with scrambled siRNA (siSCR) or siRNA molecules to knock down expression of FAS-L or FADD, as indicated. Thirty six h after transfection cells were treated with a control IgG antibody (10 mg) or with a neutralizing anti-FAS-L antibody (NOK-1). Cells were then treated with celecoxib (CEL 5.0 μM) and/or sildenafil (SIL, 2.0 μM). Twenty four h after drug treatment cells were isolated and viability determined by trypan blue exclusion assay (n = 3 +/- SEM). # $p < 0.05$ less than corresponding value in siSCR transfected cells. **(G)** BT549 in 96 well plates were pre-treated with vehicle or L-NAME (1 μM). Cells were then treated with celecoxib (CEL 5.0 μM) and/or sildenafil (SIL, 2.0 μM). Six h after treatment cells were fixed to the plate and immunohistochemistry performed to determine the plasma membrane levels of CD95. The intensity of CD95 immunostaining was determined using the Wisoft data

Accepted Article

analysis package (n = 3 +/- SEM). * $p < 0.05$ value greater than celecoxib treatment alone; # $p < 0.05$ less than corresponding value in vehicle treated cells. **(H)** HuH7 cells were transfected with either an empty vector plasmid (CMV); a plasmid to express CD95-GFP or a plasmid to express CD95-GFP-Y232F Y291F (46,47). Twenty four h after transfection cells were then treated with celecoxib (CEL 5.0 μM) and/or sildenafil (SIL, 2.0 μM). Twenty four h after drug treatment cells were isolated and viability determined by trypan blue exclusion assay (n = 3 +/- SEM). * $p < 0.05$ greater than corresponding value in CMV transfected cells.

Accepted Article

Figure 5. Sildenafil and celecoxib increase autophagy and promote ER stress which regulate the cell killing process. (A). BT549 and HOSS1 cells were transfected with a plasmid to express LC3-GFP-RFP. Twenty four h after transfection cells were then treated with celecoxib (CEL 5.0 μM) and/or sildenafil (SIL, 2.0 μM). Six h after drug treatment cells were analyzed for the numbers of GFP+ and RFP+ intense staining vesicles per cell (n = 3 +/- SEM). **(B)** BT474 cells were transfected with a plasmid to express LC3-GFP-RFP. Twenty four h after transfection cells were pre-treated with vehicle or the NOS inhibitor L-NAME (1 μM). After 30 min cells were treated with celecoxib (CEL 5.0 μM) and/or sildenafil (SIL, 2.0 μM). Twelve h after drug treatment cells were analyzed for the numbers of GFP+ and RFP+ intense staining vesicles per cell (n = 3 +/- SEM). # $p < 0.05$ less than corresponding value in vehicle treated cells; * $p < 0.05$ greater than vehicle treatment. **(C)** BT549 and HOSS1 cells were transfected with a scrambled control siRNA (siSCR) or siRNA molecules to knock down expression of Beclin1 (siBeclin1) or ATG5 (siATG5). Thirty six h after transfection cells were then treated with celecoxib (CEL 5.0 μM) and/or sildenafil (SIL, 2.0 μM). Twenty four h after drug treatment cells were isolated and viability determined by trypan blue exclusion assay (n = 3 +/- SEM). # $p < 0.05$ less than corresponding value in siSCR transfected cells. **(D)** and **(E)** BT549 and HOSS1 cells were transfected as indicated to with a scrambled siRNA (siSCR) or siRNA molecules to knock down expression of ATF6 (siATF6), XBP1 (siXBP1), IRE1α (siIRE1α), eIF2α (sieIF2α), ATF4 (ATF6), or CHOP (siCHOP). Thirty six h after transfection cells were then treated with celecoxib (CEL 5.0 μM) and/or sildenafil (SIL, 2.0 μM). Twenty four h after drug treatment cells were isolated and viability determined by trypan blue exclusion assay (n = 3 +/- SEM). # $p < 0.05$ less than corresponding value in siSCR transfected cells * $p < 0.05$ greater than corresponding value in siSCR transfected cells. Inset Panel: BT549 cells were treated with celecoxib (CEL 5.0 μM) and/or sildenafil (SIL, 2.0 μM) and isolated after 12h to determine the phosphorylation of eIF2α. **(F)** BT549 cells were transfected with an empty vector plasmid (CMV); a plasmid to express eIF2α S51A (dominant negative); a plasmid to express eIF2α S51D (activated). Twenty four h after transfection cells were then treated with celecoxib (CEL 5.0 μM) and/or sildenafil (SIL, 2.0 μM). Twenty four h after drug treatment

Accepted Article

cells were isolated and viability determined by trypan blue exclusion assay (n = 3 +/- SEM). # $p < 0.05$ less than corresponding value in CMV transfected cells * $p < 0.05$ greater than corresponding value in CMV transfected cells. **(G)** BT549 cells were transfected as indicated with a scrambled siRNA (siSCR) or siRNA molecules to knock down expression of CD95 (siCD95) or eIF2α (sieIF2α). Thirty six h after transfection cells were then treated with celecoxib (CEL 5.0 μM) and/or sildenafil (SIL, 2.0 μM). Six h after drug treatment cells were isolated and subjected to SDS PAGE and immunoblotting to determine the phosphorylation of JNK.

Accepted Article

Figure 6. Sildenafil and celecoxib interact to suppress mammary tumor growth in vivo. Panel A. BT474 cells (1 x 10^6) were injected into the 4th mammary fat pad of athymic mice and tumors permitted to form for 21 days until the mean tumor volume was ~150 mm^3. Animals were segregated into groups with very similar mean tumor volumes. Animals were treated with vehicle (cremophore), sildenafil (5 mg/kg), celecoxib (10 mg/kg) or both drugs simultaneously for 5 days QD. Tumor volumes were measured every third day and the –Fold increase in tumor volume calculated (with Day 0 = 1.00) (2 studies, 8 animals total per group +/- SEM) *p < 0.05 lower than celecoxib alone value. **Panel B.** BT474 cells (3 x 10^6) were injected into the 4th mammary fat pad of athymic mice and four days after injection animals were randomly segregated into four groups. Animals were treated with vehicle (cremophore), sildenafil (5 mg/kg), celecoxib (10 mg/kg) or both drugs simultaneously for 7 days QD. Tumor volumes were measured beginning at Day 7 and then every second day and the actual increase in tumor volume calculated (with Day 0 = 0 mm^3) (2 studies, 8 animals total per group +/- SEM) *p < 0.05 lower than celecoxib alone value. **Panel C.** BT549 cells (1 x 10^6) were injected into the 4th mammary fat pad of athymic mice and tumors permitted to form for 21 days until the mean tumor volume was ~150 mm^3. Animals were segregated into groups with very similar mean tumor volumes. Animals were treated with vehicle (cremophore), sildenafil (5 mg/kg), celecoxib (25 mg/kg) or both drugs simultaneously for 5 days QD. Tumor volumes were measured every third day and the –Fold increase in tumor volume calculated (with Day 0 = 1.00) (2 studies, 8 animals total per group +/- SEM) *p < 0.05 lower than celecoxib alone value. **Panel D.** BT549 cells (1 x 10^7) were injected into the 4th mammary fat pad of athymic mice and tumors permitted to form until the mean tumor volume was ~150 mm^3. Animals were segregated into groups with very similar mean tumor volumes. Animals were treated with vehicle (cremophore), (sildenafil (2.5 mg/kg) and celecoxib (2.5 mg/kg)) and/or FTY720 (0.05 mg/kg) simultaneously for 7 days QD. Tumor volumes were measured approximately every third day and the tumor volume calculated (with Day 0 = 1.00) (2 studies, 8 animals total per group +/- SEM) *p < 0.05 lower than celecoxib + sildenafil value. **Panel E.** Kaplan Meir survival curves based on data presented in ***Panel D.*** # greater survival that Vehicle treated animals; ## greater survival than [celecoxib + sildenafil] treatment alone.

Accepted Article

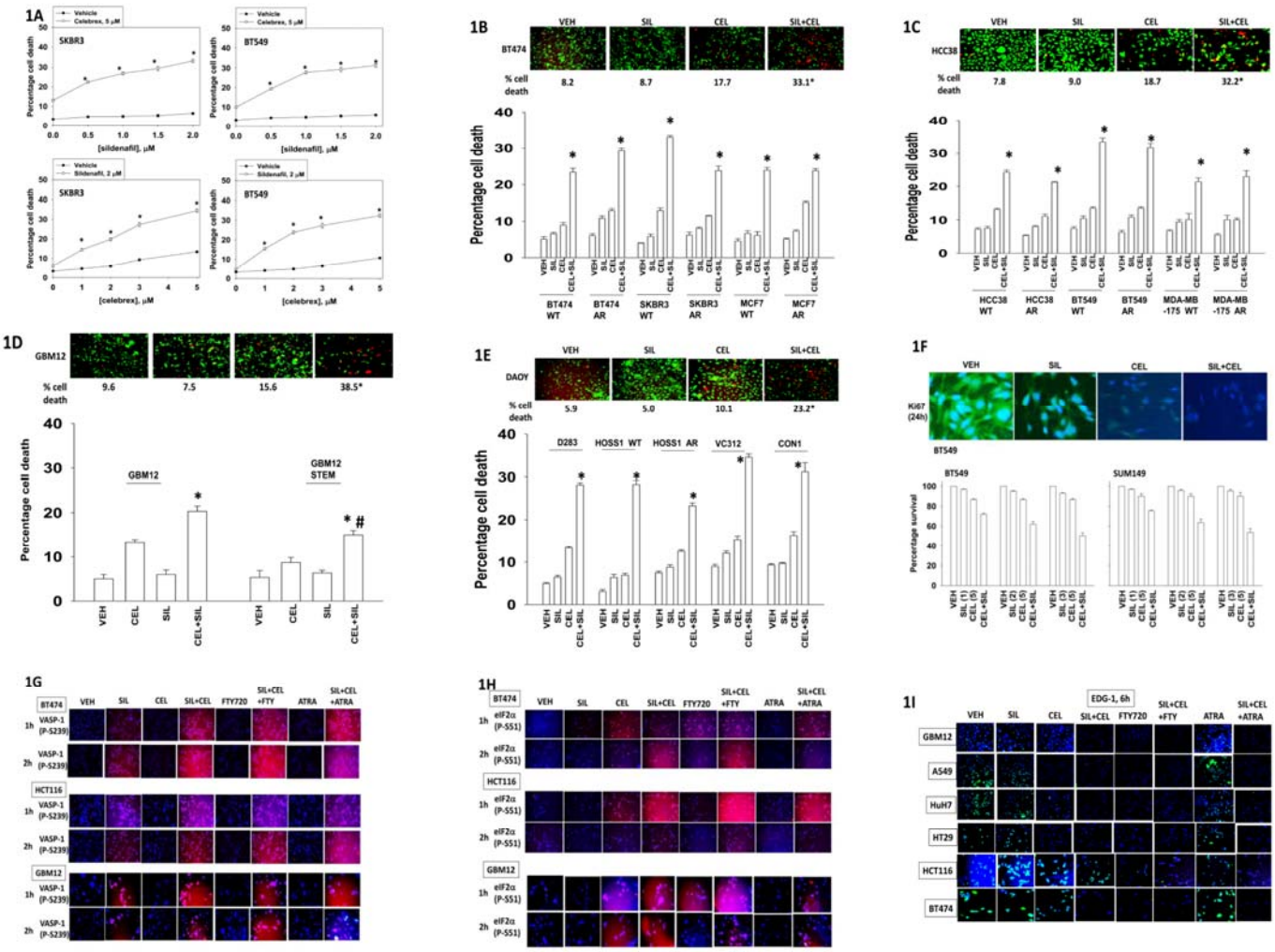

Figure 1

Accepted Article

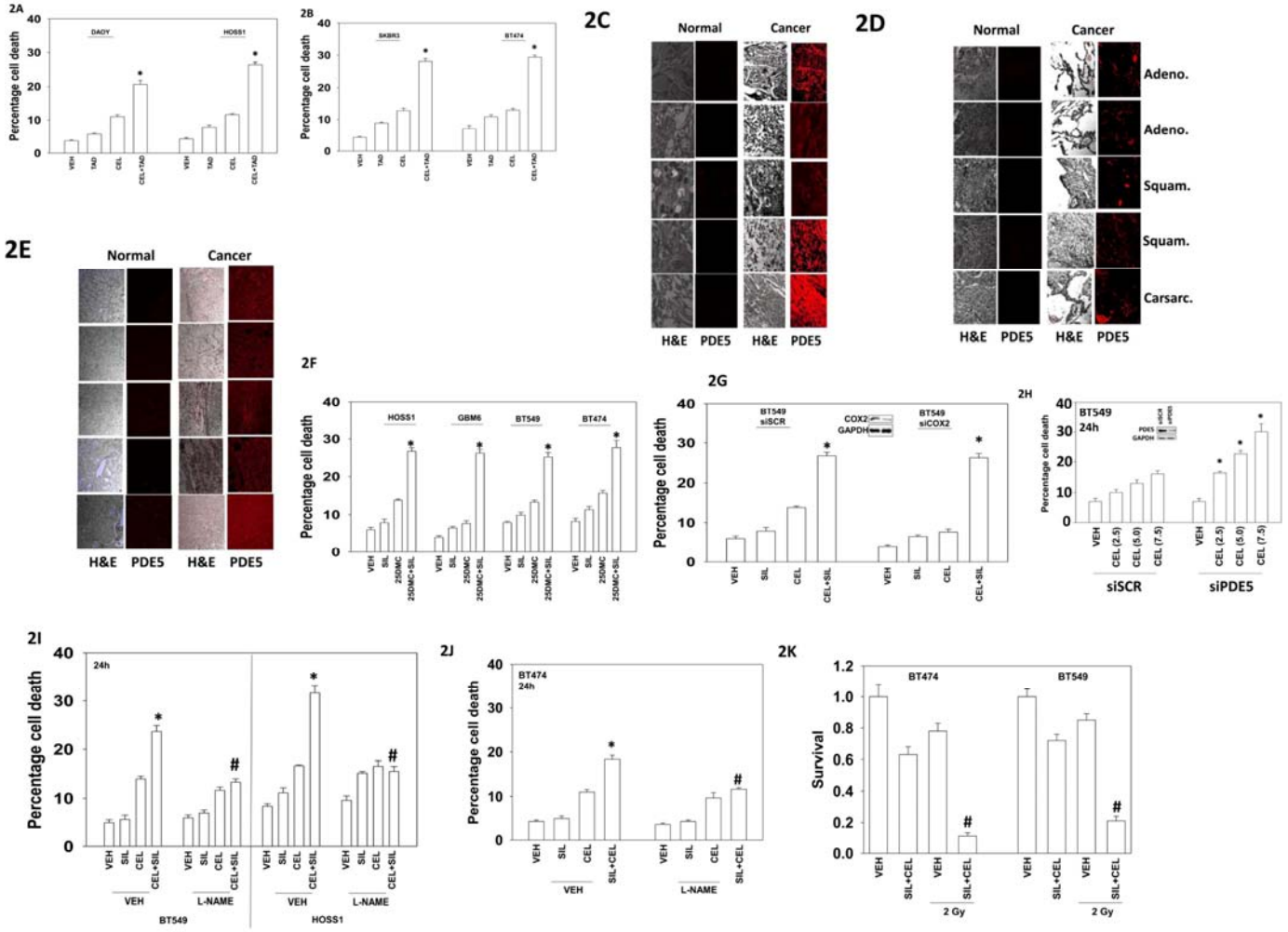

Figure 2

Accepted Article

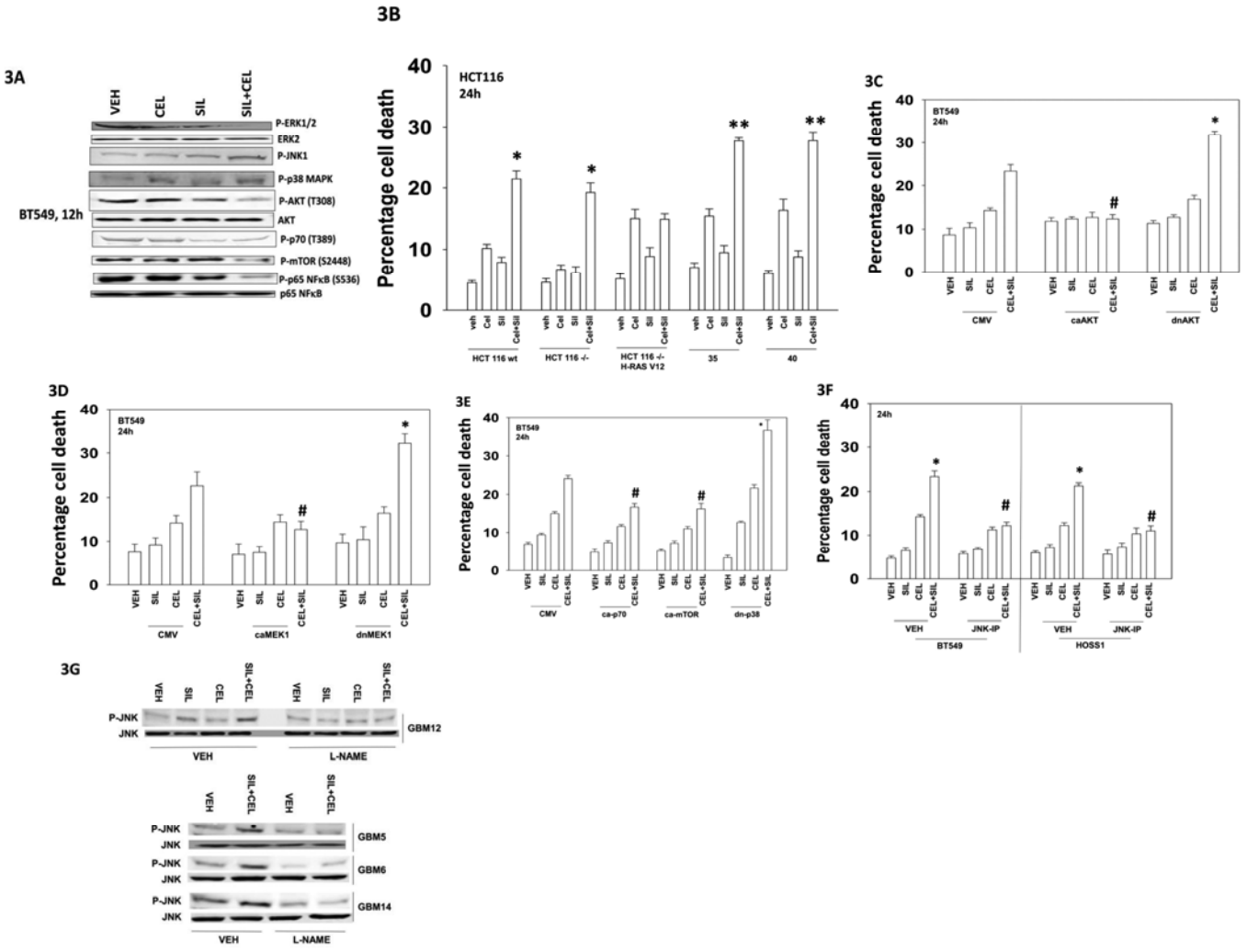

Figure 3

Accepted Article

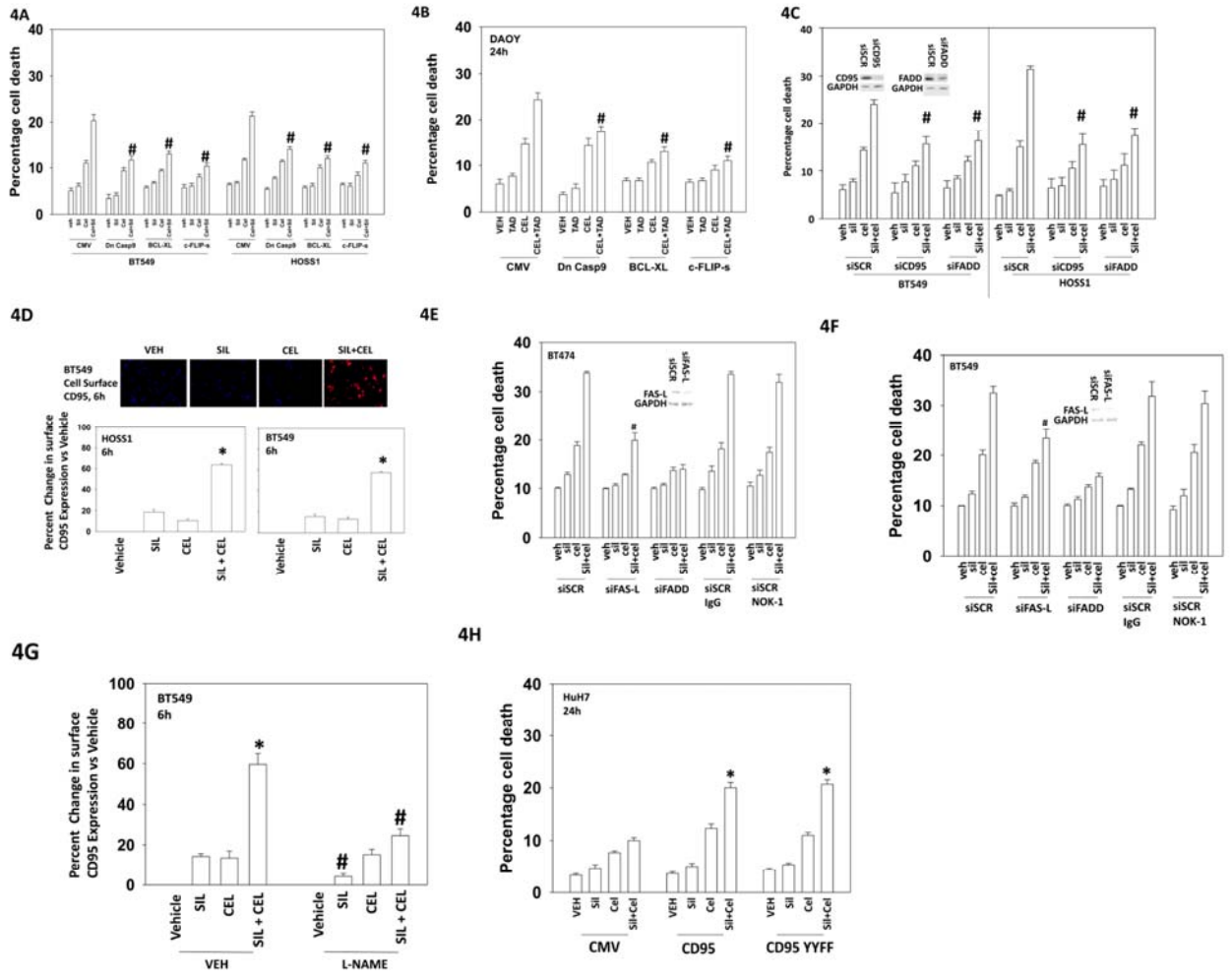

Figure 4

Accepted Article

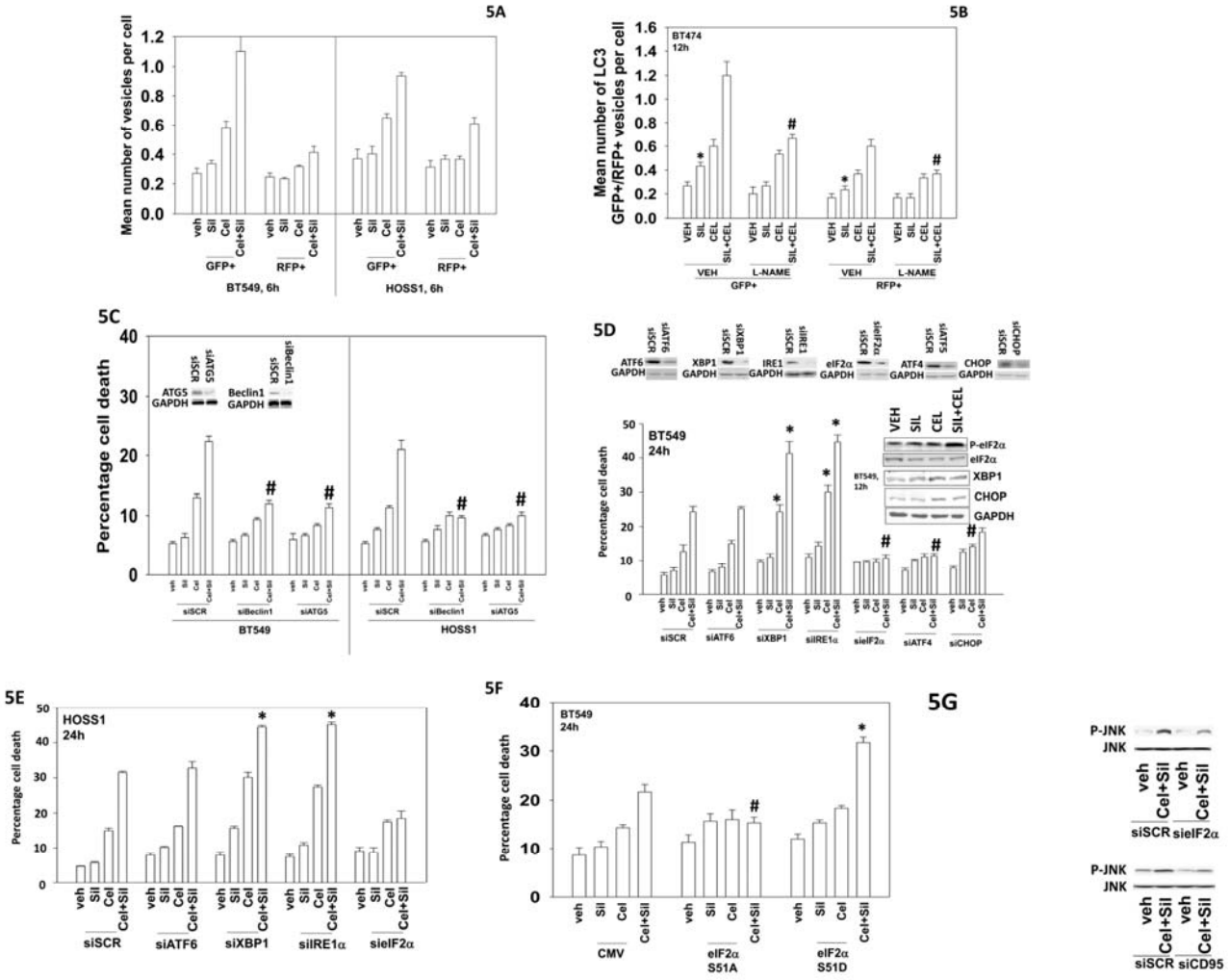

Figure 5

Accepted Article

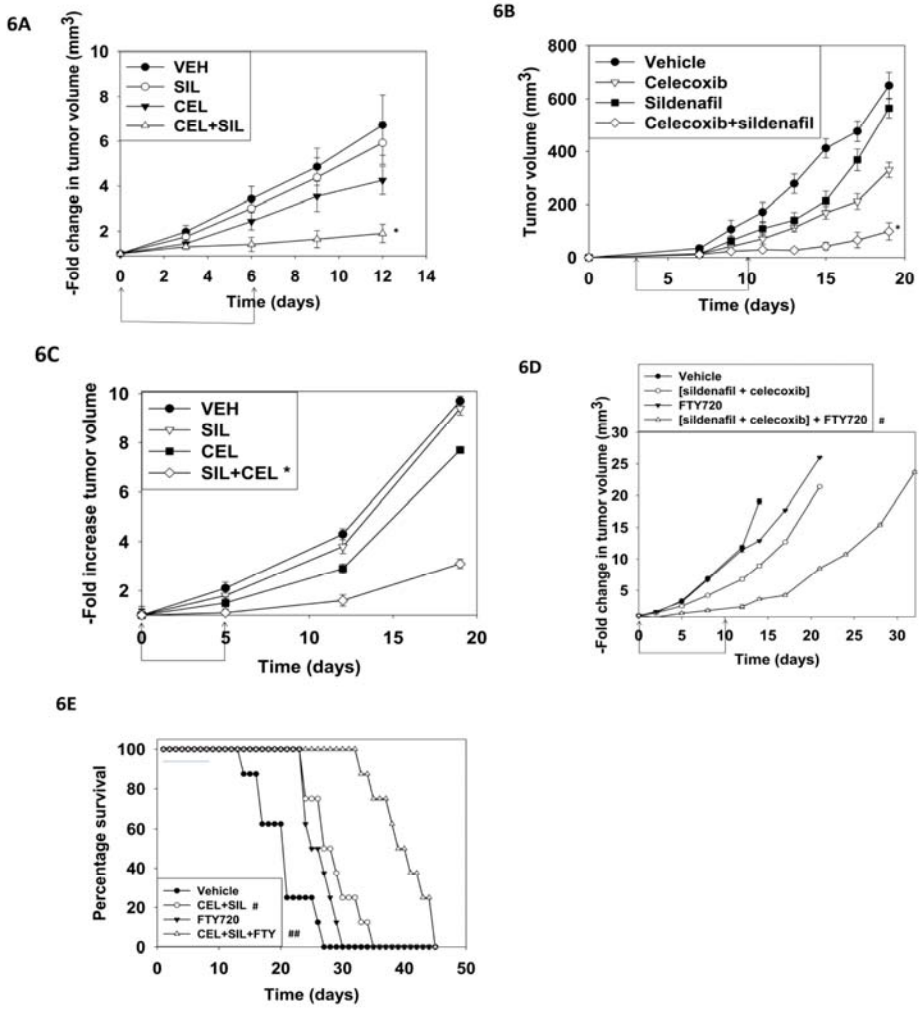

Figure 6

Accepted Article